M2 microglia and macrophages drive oligodendrocyte differentiation during CNS remyelination

Nature Neuroscience 16, 1211–1218 (2013) doi:10.1038/nn.3469

Nature Neuroscience: Article

Title:

M2 microglia/ macrophages drive oligodendrocyte differentiation during CNS remyelination

Authors:

Veronique E. Miron[1], Amanda Boyd[1], Jing-Wei Zhao[2], Tracy J. Yuen[1,2], Julia M. Ruckh[2], Jennifer L. Shadrach[3], Peter van Wijngaarden[2], Amy J. Wagers[3], Anna Williams[1], Robin J.M. Franklin[2 *] & Charles ffrench-Constant[1*]

* joint senior authors contributed equally to this manuscript

Affiliations:
1. MRC Centre for Regenerative Medicine/ MS Society Centre for Translational Research, University of Edinburgh, Edinburgh, UK.

2. Wellcome Trust and MRC Cambridge Stem Cell Institute and Department of Veterinary Medicine, University of Cambridge, Cambridge, UK.

3. Howard Hughes Medical Institute and Department of Stem Cell and Regenerative Biology, Harvard University, Harvard Stem Cell Institute & Joslin Diabetes Center, Cambridge, USA.

Corresponding author:

Veronique E. Miron

MRC Centre for Regenerative Medicine

The University of Edinburgh

Edinburgh BioQuarter

5 Little France Drive

Edinburgh

EH16 4UU

Tel: +44 (0) 131 651 9570

Fax: +44 (0) 131 651 9501

Email: vmiron@staffmail.ed.ac.uk

Word count: Text 2995; Figure Legends 1268; Methods 2659; References 48

Figures: 8

Supplemental Figures: 9

Supplemental Tables: 1

Nature Neuroscience 16, 1211–1218 (2013) doi:10.1038/nn.3469

The lack of therapies for progressive multiple sclerosis highlights the need to understand the regenerative process of remyelination that can follow CNS demyelination. This involves an innate immune response consisting of microglia/ macrophages, which can be polarized to distinct functional phenotypes: pro-inflammatory (M1) or anti-inflammatory/ immunoregulatory (M2). Here we show that a switch from an M1- to M2-dominant response occurred within microglia and peripherally-derived macrophages as remyelination started. Oligodendrocyte differentiation was enhanced *in vitro* with M2 conditioned media, and impaired *in vivo* following intra-lesional M2 depletion. M2 densities were increased in lesions of aged mice in which remyelination was enhanced by parabiotic coupling to a younger animal, and in MS lesions that normally show remyelination. Blocking M2-derived activin-A inhibited oligodendrocyte differentiation during remyelination in cerebellar slice cultures. Our results therefore show that M2 polarization is essential for efficient remyelination and identify activin-A as a novel therapeutic target for CNS regeneration.

Remyelination, the formation of myelin sheaths around demyelinated axons by newly differentiated oligodendrocytes, can occur efficiently following central nervous system (CNS) demyelination. A major component of this regenerative process is a robust innate immune response consisting of peripherally-derived macrophages and their CNS-resident counterparts, microglia. Although these microglia/ macrophages are implicated in CNS autoimmune disease via secretion of toxic molecules [1] and antigen presentation to cytotoxic lymphocytes [2], they also exhibit regenerative properties through the phagocytosis of myelin debris [3, 4] and secretion of growth/neurotrophic factors [5]. Regenerative properties of microglia/ macrophages following injury to muscle [6, 7] and skin [8] are associated with alternative or de-activation to M2-polarized phenotypes (M2a and M2c, respectively), which secrete anti-inflammatory cytokines/ growth factors [9]. In contrast, M1 'classically activated' phenotypes are associated with enhanced antigen presentation properties and secretion of pro-inflammatory cytokines and reactive oxygen/nitrogen species [9]. In this study, we therefore explored the role of microglia/ macrophage polarization in remyelination, asking whether M2 phenotypes contribute to this regenerative response in the CNS and whether a study of M2-derived factors could lead to the identification of a novel target for remyelination therapies.

Results

An M1 to M2 switch at the initiation of remyelination.

To examine the timing of microglia/ macrophage polarization during remyelination, we induced focal demyelination by stereotaxic injection of lysolecithin into the mouse corpus callosum. Tissue was analyzed at 3, 10, and 21 days post lesion (dpl), times that correspond to key steps in the remyelination process: oligodendrocyte progenitor cell (OPC) recruitment into the lesion by proliferation and migration, initiation of remyelination by the differentiation of these OPCs into myelin-sheath forming oligodendrocytes, and completion of remyelination (**Fig. 1a**) [10-13]. Studies of microglia/ macrophages with polarization state-specific markers revealed a switch from an M1- to M2-dominant phenotype at the initiation of remyelination. At 3 dpl, substantially more CD68+ microglia/ macrophages expressed the M1 marker inducible nitric oxide synthase (iNOS) than the M2 marker arginase-1 (Arg-1) (**Fig. 1b, c**). However, by 10 dpl there were more Arg-1+ CD68+ M2 cells than iNOS+ CD68+ M1 cells (**Fig. 1b, c**). At 21 dpl, there was a reduction in Arg-1+ M2 cells compared to 10 dpl (**Fig. 1b, c**). Only a low percentage of CD68+ microglia/ macrophages remained unpolarized (iNOS– and Arg-1–) throughout remyelination (**Fig. 1c**). The polarization switch during remyelination was confirmed using additional markers for M1 (tumor necrosis factor (TNF)α and CD16/32) and M2 phenotypes (mannose receptor (MR) and insulin-like growth factor (IGF)-1) (**Supplementary Fig. 1 online**). We also observed the same switch from an M1 to M2 response during remyelination in another model of demyelination induced by injection of ethidium bromide into the rat caudal cerebellar peduncles (CCP) (**Supplementary Fig. 2 online**) [14].

As the entry of peripherally-derived macrophages to function alongside CNS-resident microglia is an important part of the innate immune response in the CNS [5, 15, 16], we next determined whether this switch in polarization phenotype was a consequence of a change in the balance of (differentially-polarized) endogenous microglia vs. peripherally-derived macrophages, or of polarization switching in both populations. To exclude macrophages from lesions and therefore examine polarization only in microglia, we examined lesions created in C-C chemokine receptor 2 $(CCR2)^{-/-}$ mice whose peripheral monocytes (from which macrophages derive) cannot extravasate [4, 17] and are thus excluded from entering remyelinating lesions [4] (**Fig. 2a**). The transition from M1 to M2 polarization still occurred as before within the microglia population in $CCR2^{-/-}$ mice, with the majority of CD68+ cells being iNOS+ at 3 dpl and Arg-1+ at 10 dpl (**Fig. 2b**, **c**). However, the absence of peripherally-derived macrophages in $CCR2^{-/-}$ lesions did lead to a reduction in total numbers of iNOS+ M1 cells (to 37 ± 10 and 33 ± 7 % of wildtype control at 3 and 10 dpl, respectively) and Arg-1+ M2 cells (to 8 ± 8 and 40 ± 13 % of wildtype controls at 3 and 10 dpl, respectively). To examine polarization only in peripherally-derived macrophages within a lesion, green fluorescent protein (GFP)-expressing wildtype bone marrow-derived cells were injected into the circulation of lesioned $CCR2^{-/-}$ mice (**Fig. 2d**). Both GFP+ iNOS+ M1 macrophages and GFP+ Arg-1+ M2 macrophages were present at 3 and 10 dpl (**Fig. 2e**, **f**). The iNOS+ M1 population was composed of 39 ± 3 % (3 dpl) and 46 ± 14 % GFP+ macrophages (10 dpl) whereas the Arg-1+ M2 population was composed of 63 ± 12 % (3 dpl) and 68 ± 23 % GFP+ macrophages (10 dpl), showing that macrophages contribute equally to both M1 and M2 populations before and during the switch in polarization. We conclude, therefore, that both peripherally-derived

macrophages and resident microglia contribute to the switch from M1 to M2 phenotypes that we observed at the initiation of remyelination.

M2 microglia promote oligodendrocyte differentiation.

The switch from M1 to M2 polarization at 10 dpl led us to hypothesize that the two polarization states may have distinct roles in regulating the oligodendrocyte differentiation essential for the initiation of remyelination that occurs at this time. To test this, we first assessed the responses of OPCs to application of M1 and M2 conditioned media *in vitro*. We used microglia rather than peripherally-derived macrophages since the former are always a component of the innate immune response regardless of changes to the blood-brain barrier, and we had confirmed above that microglia alone can undergo the switch in polarization *in vivo*. Microglia were polarized to M1 or one of two M2 subtypes (M2a (anti-inflammatory) and M2c (immuno-regulatory)) by exposure to interferon (IFN)-γ/ lipopolysaccharide (LPS), interleukin (IL)-13, and IL-10, respectively (**Supplementary Fig. 3 online**). We examined polarization by immunofluorescence, enzyme-linked immuno-absorbant assay (ELISA), and by gene expression profiling, confirming that the phenotypes matched those measured *in vivo* during remyelination [18] (**Supplementary Fig. 3 and 4 online**).

Conditioned media derived from both M1 and M2 microglia increased OPC proliferation (evidenced by increased total OPC numbers, cell cycle activity, and 5-bromo-2-deoxyuridine (BrdU) incorporation (**Supplementary Fig. 5a-d online**)) and also increased chemotaxic migration (**Supplementary Fig. 5e online**). In contrast, only M2 conditioned media prevented OPC apoptosis in media deprived of serum and

growth factors (**Supplementary Fig. 6 online**), conditions that reveal the physiological target-dependent survival mechanisms of newly-formed oligodendrocytes *in vivo.* Additionally, only M2 conditioned media increased oligodendrocyte differentiation, assessed by expression of myelin basic protein (MBP) (**Fig. 3a, b**) and myelin oligodendrocyte glycoprotein (MOG) (**Fig. 3c**).

M2 depletion inhibits oligodendrocyte differentiation.

Having revealed distinct effects of M1 and M2 conditioned media in cell culture, with only M2 conditioned media enhancing oligodendrocyte differentiation, we next determined the effect of selective depletion of each polarized macrophage population during remyelination *in vivo*. We depleted M1 cells by administration of gadolinium chloride ($GdCl_3$) within a lesion, which upon phagocytosis induces apoptosis of inflammatory macrophages via competitive inhibition of Ca^{2+} mobilization and damage to plasma membranes [19-22]. We confirmed the ability of GdCl3 (270 μM) to selectively deplete M1 cells *in vitro* (**Supplementary Fig. 7a-c online**) and within a lesion *in vivo* by injection at the time of lesioning (**Fig. 4a-c** and **Supplementary Fig. 7e**, **f online**). GdCl3 injection did not significantly affect M2 cell numbers (**Fig. 4c**). M1 depletion reduced the density of proliferating cell nuclear antigen (PCNA)+ Nkx2.2+ proliferating OPCs at 3dpl compared to control (**Fig. 4d**), confirming a role for M1 polarization in regulating OPC proliferation. However, OPC migration (as measured by numbers of NG2+ or Nkx2.2+ OPCs) and remyelination were not impaired (**Supplementary Fig.7g**, **h online**).

We depleted M2 cells using mannosylated clodronate liposomes (MCLs) that bind the mannose receptor (**Fig. 5a**) which is upregulated following M2 polarization

(**Supplementary Fig. 3 online**), and induce apoptosis within 2–3 days via clodronate-mediated depletion of intracellular iron [23, 24]. We confirmed selective M2 depletion *in vitro* (**Supplementary Fig. 8a-f online**) and *in vivo* when MCLs were injected into a lesion at 8 dpl (**Fig. 5b-d** and **Supplementary Fig. 8g, h online**). M2 depletion caused an increase in the number and proportion of iNOS+ M1 cells (**Fig. 5d** and **Supplementary Fig. 8g online**), supporting previous findings of reciprocal regulation between M1 and M2 polarization and associated cytokines [25, 26]. M2 depletion decreased expression of differentiation markers myelin associated glycoprotein (MAG) and MBP at 10 dpl (**Fig. 5e, f**), indicating a delay in oligodendrocyte differentiation. We measured the consequent delay in remyelination in tissue at 21 dpl following M2-depletion in two different ways. First, we observed decreased co-localization of MBP and the late myelin marker MOG (**Supplementary Fig. 8i online**). Second, we demonstrated a decrease in the number of nodes of Ranvier normally indicative of compact myelin [27, 28] by showing reduced paranodal Caspr localization (flanking nodal Ankyrin-G) (**Fig. 5g, h**). No change was observed in lesion area (data not shown), numbers of Nkx2.2+ OPCs, presence of neurofilament (NF)+ axons, and glial fibrillary acidic protein (GFAP)+ astrocyte reactivity within the lesion (**Supplementary Fig. 8j-l online**).

Increased M2 densities during efficient remyelination.

These *in vivo* depletion experiments show that a switch to an M2 dominant phenotype in demyelinated lesions is required for efficient remyelination. We would predict, therefore, that experimental manipulations leading to increased numbers of M2 macrophages would enhance remyelination. To confirm this, we examined parabiosis experiments where the slow remyelination normally observed in old mice can be

reversed by sharing a circulation with young mice [4], an effect mediated in part by recruitment of young circulating monocytes into the demyelinating lesions of the older mice. We analyzed previously-characterized tissue of lysolecithin-demyelinated ventral spinal cord of one of the two mice in various pairings [4] (**Fig. 6a**). Densities of M2 microglia/ macrophages (MR+ isolectin B4+ and Arg-1+ CD68+) were higher in the lesions of young animals paired to another young animal (Y/Y) than in old animals paired to another old animal (O/O) (**Fig. 6b, c**). Pairing of an old animal with a young animal (Y/O), a manipulation that restores remyelination efficiency in the older animal [4], led to increased densities of M2 microglia/ macrophages in the lesions in the older animal relative to those seen in the O/O pairings (**Fig. 6b, c**). In contrast, densities of CD16/32+ M1 microglia/ macrophages were substantially higher in O/O pairings than Y/Y pairings and not significantly reduced by Y/O pairing (**Fig. 6d**). Thus, increasing densities of M2 microglia/ macrophages is associated with enhanced remyelination efficiency. When we analyzed parabiosis experiments between a GFP-expressing young mouse and a lesioned wild type old mouse [4] so as to assess the contribution of peripherally-derived young macrophages (GFP+) to the M1 and M2 polarized populations within a remyelinating lesion (**Fig. 6e**), GFP+ iNOS+ CD68+ M1 macrophages and GFP+ Arg-1+ CD68+ M2 macrophages present within the lesion (**Fig. 6f**) only contributed to 3.6 ± 1.6 % of iNOS+ M1 cells and 12.4 ± 5 % of Arg-1+ M2 cells. The great majority of the increased numbers of M2 cells in the older animal of the Y/O pairings must therefore have derived from the microglia/ macrophages of the old animal, with the young macrophages that enter the lesion in the old CNS rejuvenating the lesion environment to promote M2 polarization of endogenous populations.

A second prediction of our conclusion that a switch to an M2-dominant phenotype in demyelinated lesions is required for efficient remyelination, and one critical for translational relevance, is that M2 macrophages will be abundant in areas of multiple sclerosis (MS) lesions associated with ongoing remyelination. To test this, we examined 5 patterns of MS lesion pathology (acute active, rim of chronic active, centre of chronic active, chronic inactive, remyelinated; **Supplemental Table 1**). All lesion types showed significantly higher densities of total CD68+ microglia/ macrophages and iNOS+ M1 cells compared to controls (**Fig. 7d, f**). While a few remyelinated lesions showed increased densities of MR+ M2 cells compared to controls, significantly elevated numbers of M2 cells were seen only in acute active lesions and within the rim of chronic active lesions (**Fig. 7e, f, g**), both areas of recent damage where ongoing remyelination would be expected.

M2-derived activinA drives oligodendrocyte differentiation.

Together, our data indicate that the switch to M2 polarization is an essential part of the regenerative response in the CNS by promoting oligodendrocyte differentiation. To identify an M2-derived regenerative factor, we took a candidate approach and investigated the transforming growth factor (TGF) β superfamily member activin-A in light of its neuroprotective properties [29, 30], and the upregulation of its receptor (*Acvr2b*) during remyelination [18]. Activin-A is produced by inflammatory macrophages and is a marker of M2 polarization [31, 32]. In keeping with this, we found that more MR+ M2a and M2c polarized microglia expressed activin-A *in vitro* in comparison to iNOS+ M1 microglia (**Fig. 8a**). To confirm that M2 polarized cells also contribute activin-A to the environment of remyelinating lesions, we examined expression in lesions and found that activin-A immunoreactivity was more evident in

association with MR+ M2 cells at 10 dpl compared to iNOS+ M1 cells at 3 dpl, and was reduced upon M2 depletion with MCLs (**Fig. 8b**). Examination of expression of receptors that directly bind activin-A, Acvr2A and Acvr2B, showed that NG2+ OPCs within remyelinating lesions expressed both subtypes (**Fig. 8c**). Importantly, OPCs also expressed Acvr1B, the receptor which is recruited by ligand-bound Acvr2 and which is required for subsequent functional downstream signalling [33]. Together, these findings indicate the capacity of OPCs within remyelinating lesions to directly bind and respond to M2-derived activin-A. Assessment of activin-A binding capacity of other cell types within lesions indicates that Acvr2 is expressed by CC1+ oligodendrocytes (Acvr2B+) and CD68+ microglia/ macrophages (Acvr2A+, Acvr2B+), but not by GFAP+ astrocytes or NF+ axons (**Supplementary Fig. 9 online**).

To test the effect of activin-A on oligodendrocyte differentiation, we exposed cultured OPCs to activin-A and found it was sufficient to enhance oligodendrocyte differentiation (**Fig. 8d**). To confirm a role for activin-A in the differentiation-promoting effect of M2 microglia, we supplemented cultures with M2 conditioned media and an activin-A blocking antibody and observed reduced oligodendrocyte differentiation (MBP+ cells) (**Fig. 8e**). Given that activin-$A^{-/-}$ mice are neonatally lethal, and activin receptor null mutants are either developmentally lethal or have gastrulation and fertility defects [34, 35], we investigated the role of activin-A in M2-driven oligodendrocyte differentiation during remyelination in intact CNS using *ex vivo* organotypic cerebellar slice cultures (**Fig. 8f**). Following lysolecithin-induced demyelination, slices treated with M2 CM during the initiation of remyelination showed increased numbers of CC1+ MBP+ mature oligodendrocytes, which was

considerably reduced with anti-activin-A blocking IgG supplementation (**Fig. 8g, h**). This was due to blocking of activin-A in M2 conditioned media and not endogenous activin-A, as treatment of slices with anti-activin-A antibody alone did not reduce the number of oligodendrocytes relative to IgG control (**Fig. 8h**). Together, these data provide a molecular mechanism for M2-driven oligodendrocyte differentiation during remyelination via secretion of activin-A.

Discussion

Our results showed that a switch occurs from M1 to M2 polarization in both resident microglia and peripherally-derived macrophages in CNS lesions during remyelination. This switch occurs at 10 dpl corresponding to the time of differentiation of oligodendrocytes derived from OPCs that have been recruited into the lesion. Using cell culture, *in vivo* manipulation of macrophage populations, parabiosis experiments and correlative analysis of human MS lesions, we showed that M2 microglia/ macrophages drive oligodendrocyte differentiation during remyelination and that this is an essential part of an effective remyelination response.

A switch from M1- to M2-associated gene expression has been reported during cutaneous wound healing [8] but has not been observed in studies of immune-mediated [36] and toxin (cuprizone)-induced demyelination [37]. This failure to observe a switch in different models of remyelination likely reflects the confounding effects of overlapping de- and remyelination phases in these models, and the consequent difficulty in establishing any correlation with the different stages of the regenerative process. Our choice of lesion model is the most appropriate to overcome this issue, as damage occurs at the time of toxin injection after which only the regenerative process is present.

We have also shown, using organotypic cerebellar slice cultures, that this M2-driven regenerative response is mediated at least in part by secretion of the TGFβ superfamily member, activin-A. In accordance with our finding, signalling pathways downstream of activin receptor activation include Rac/Cdc42 GTPases, Akt, and mammalian target of rapamycin (mTOR), all of which have been previously

implicated in positively regulating oligodendrocyte differentiation and/or myelination [38-41]. Additionally, TGFβ isoforms have been shown to induce myelin protein expression [42, 43]. Our novel finding implicating activin-A in the regulation of oligodendrocyte differentiation together with evidence of activin-A's neuroprotective properties [29, 30], the expression of its receptors on OPCs in remyelinating lesions, and the upregulation of its receptor during remyelination [18], highlights this factor as a promising novel therapeutic target for CNS myelin regeneration.

Whereas previous studies investigating microglia/ macrophage polarization in the context of neuronal injury have highlighted the neuroprotective properties of M2 cells [44, 45], in this study we have identified the regenerative capacity of M2 cells in the CNS. Our results showing that M2 cells are required for oligodendrocyte differentiation are of particular interest given that a block in oligodendrocyte differentiation is a feature of chronic MS lesions [46]. Our results also have implications for the use of immuno-modulatory MS therapies; the CNS-permeable therapy FTY720 decreases peripheral M1 and M2 polarization in rodents [47], whereas glatiramer acetate induces a peripheral M2 phenotype [48], although any effect on central M2 polarization remains undetermined. We suggest that cell- or drug-based therapies founded on manipulating M2 polarization and/or activin-A expression in the CNS represent complementary regenerative strategies that may support remyelination and clinical recovery in MS.

Acknowledgements

We thank the United Kingdom Multiple Sclerosis Tissue Bank for providing human brain tissue, Dr. F. Roncaroli (Imperial College London) for neuropathological diagnosis of lesions, and Dr. R. Nicholas (Imperial College London) for providing clinical history of patients. We also thank William Mungall, Jeffrey Huang, Marie Harrisingh, Andrew Jarjour, Marie Bechler, Ana-Cristina Nunes-Fonseca, Daniel Morrison, and Corrie Watkins for technical assistance. This work was funded by the United Kingdom Multiple Sclerosis Society (R.J.M.F., C.ff.-C.) and Wellcome Trust (A.W., C.ff.-C.), and V.E.M. holds a post-doctoral fellowship from the Multiple Sclerosis Society of Canada.

Author Contributions

V.M. conceived the project, designed and carried out experiments, performed data acquisition, quantification, and analysis, and wrote the manuscript; A.B. and A.W. assisted in *in vivo* studies, and A.W. assisted in data interpretation; J.-W.Z. contributed to analysis and quantification of parabiosis lesion tissue; A.B., A.W., T.Y., and P.v.W. performed lesioning experiments to provide lesion tissue and assisted in tissue selection; J.R., J.S., A.J.W, R.J.M.F. provided parabiosis lesion tissue; R.J.M.F. assisted in study design, data interpretation, and manuscript writing; C.ff.-C. supervised the project, assisted in study design, data interpretation, figure preparation, and writing of the manuscript.

Figure Legends

Figure 1 A switch from an M1 to an M2-dominant microglia/macrophage response occurs at the initiation of remyelination.

(a) Oligodendroglial lineage cell responses in the corpus callosum at 3, 10, and 21 days post lesion (dpl) induction by stereotactic injection of lysolecithin (LPC). (b) Lesions immunostained against iNOS (green), Arg-1 (red), and CD68 (white) at 3, 10 and 21 dpl. Inset: isotype controls. Scale bar, 25 μm. (c) Percentage of iNOS+ M1 cells, Arg-1+ M2 cells, and iNOS–Arg-1– (unpolarized) cells per field in lesion ± s.e.m.. One way ANOVA and Newman-Keuls post-hoc test, ***p<0.001 (*n*=5 mice, df=44).

Figure 2 Microglia and peripherally-derived macrophages contribute to both M1 and M2 polarized populations during remyelination.

(a) *Ccr2*$^{-/-}$ mice were lesioned in the corpus callosum to examine polarization in microglia only. (b) *Ccr2*$^{-/-}$ lesions at 3 and 10 dpl immunostained against iNOS (green), Arg-1 (red) and CD68 (white). Scale bar, 25 μm. (c) Percentage of iNOS+, Arg-1+, or unpolarized (iNOS–, Arg-1–) cells in *Ccr2*$^{-/-}$ lesions ± s.e.m.. One way ANOVA and Newman-Keuls post-hoc test, ***p<0.001 (*n*=2-3 mice, df=14). (d) *Ccr2*$^{-/-}$mice were lesioned in the corpus callosum and injected with GFP-expressing wildtype bone marrow derived cells to examine polarization in peripherally-derived macrophages only. (e) GFP+ macrophages (stars) and GFP– microglia (hash symbols) were iNOS+ (white) or Arg-1+ (red). Scale bar, 5 μm. (f) Numbers of GFP+ (macrophages) (black bars) and GFP– (microglia)(white bars) iNOS+ M1 and Arg-1+ M2 cells per field ± s.e.m. (*n*=3 mice).

Figure 3 M2 conditioned media promotes oligodendrocyte differentiation.

(a) OPCs treated with unconditioned (control) or M1, M2a, or M2c conditioned media immunostained against NG2 (green) and MBP (red). Scale bar, 50 μm. (b) Percentage of MBP+ cells ± s.e.m. following treatment with microglia conditioned media, or polarizing factors alone as a control., Kruskal-Wallis test and Dunn's multiple comparison post-test, ***p<0.001 (*n*=3 separate experiments). (c) Number of MOG+ cells per field ± s.e.m. following treatment with microglia conditioned media. Kruskal-Wallis test and Dunn's multiple comparison post-test, **p<0.01 (*n*=3 separate experiments).

Figure 4 Selective depletion of M1 microglia/ macrophages in a demyelinated lesion in the CNS impairs OPC proliferation.

(a) Gadolinium chloride (GdCl3) was injected into corpus callosum lesions at the onset of demyelination (0 dpl) prior to the peak in M1 polarization at 3 dpl. (b) Representative images of control or GdCl3-injected lesions at 3 dpl with immunostaining against iNOS (green), Arg-1 (red), and CD68 (white). Scale bar, 25 μm. (c) Numbers of iNOS+ M1, Arg-1+ M2, or unpolarized (iNOS–, Arg-1–) cells per field ± s.e.m. in control and GdCl3-injected lesions at 3 dpl. One way ANOVA and Newman-Keuls post-test, **p<0.01 (*n*=5 mice, df=29). (d) Density of PCNA+ Nkx2.2+ proliferating OPCs per mm^2 in control and GdCl3-injected lesions ± s.e.m. at 3 dpl. *P*=0.0496, 2-tailed Student's *t*-test (*n*=5 mice, df=8).

Figure 5 Selective depletion of M2 microglia/ macrophages in a demyelinated lesion in the CNS impairs oligodendrocyte differentiation.

(a) Mannosylated clodronate liposomes were used to induce apoptosis selectively in M2 polarized microglia/ macrophages due to upregulation of mannose receptor, and induce clodronate-mediated apoptosis following phagocytosis. (b) Corpus callosum lesions were injected with MCLs at 8 dpl prior to the peak in M2 polarization at 10 dpl. (c) Representative images at 10 dpl of control and MCL-injected lesions immunostained for iNOS (green), Arg-1 (red), and CD68 (white). Scale bar, 25 μm. (d) Number of iNOS+ M1, Arg-1+ M2, or unpolarized (iNOS–, Arg-1–) cells per field ± s.e.m. in control and MCL-injected lesions at 10 dpl. One way ANOVA and Newman-Keuls post-test, **p<0.01, ***p<0.001 (*n*=5 mice, df=29). (e) Mean lesion pixel counts ± s.e.m. for MAG and MBP at 10 dpl. 2-tailed Student's *t*-test versus control, *P*=0.0361 and 0.0106, respectively (*n*=4-5 mice, df=7). (f) Representative images of lesions (dotted outline) at 10 dpl in control and MCL-injected lesions immunostained against MBP (red) and MAG (green). Scale bar, 100 μm. (g) Quantification of nodes of Ranvier (paranodal Caspr expression flanking nodal Ankyrin-G expression) ± s.e.m. in control and MCL-treated lesions at 21 dpl. 2-tailed Student's *t*-test versus control, *P*=0.0068 (*n*=6 mice, df=10). Box plots indicate median (centre line), 25^{th} -75^{th} percentile (box limits) and minimum and maximum (whiskers). (h) Representative images of control and MCL-treated lesions at 21 dpl immunostained against Caspr (green) and Ankyrin-G (red). Scale bar, 25 μm.

Figure 6 Restored remyelination efficiency in aged mice via heterochronic parabiosis is associated with increased densities of M2 polarized cells.

(a) Lesion induction in the ventral spinal cord by lysolecithin injection. Parabiotic pairings between young (Y-Y) (white) or old (O-O) (dark gray) animals were compared to lesions in old animals following heterochronic pairing (Y-O) (light gray), with previous studies showing restored remyelination efficiency in old partners of Y-O pairings. (b) Lesions immunostained at 7 dpl against Arg-1 (red) and CD68 (white). Scale bar, 25 μm. (c) MR+ IB4+ M2 cells/ 0.1 mm^2 ± s.e.m. at 7 dpl. 2-tailed Student's *t*-test: Y/Y vs. O/O, *P*=0.048; Y/O vs. O/O, *P*=0.005 (*n*=4 (O/O), 6(Y/O), 4 (Y/Y), df=13). (d) CD16/32+ IB4+ cells/0.1 mm^2 ± s.e.m. at 7 dpl. 2-tailed Student's *t*-test: Y/Y vs. O/O, *P*=0.0027; Y/Y vs. Y/O, *P*=0.014 (*n*=4 (O/O), 6(Y/O), 4 (Y/Y), df=13). (e) Parabiosis between a GFP–expressing young mouse and wildtype (WT) old mouse with a spinal cord lesion. (f) GFP expressing iNOS+ CD68+ M1 macrophages and Arg-1+ CD68+ M2 macrophages. Scale bar, 5 μm.

Figure 7 M2 microglia/ macrophage densities are increased in acute active and the rim of chronic active multiple sclerosis lesions.

(a) Total CD68+ microglia/ macrophages/ mm^2 were significantly increased in acute active (*P*=0.001), chronic active rim (*P*=0.0156) and centre (*P*=0.0156), chronic inactive (*P*=0.001) and remyelinated lesions (*P*=0.002). (b) iNOS+ M1 microglia/ macrophages/ mm^2 were increased in acute active (*P*=0.001), chronic active rim (*P*=0.0156) and centre (*P*=0.0313), chronic inactive (*P*=0.0005), and remyelinated lesions (*P*<0.0001). (c) MR+ M2 microglia/ macrophages / mm^2 were increased in acute active lesions (*P*=0.0068) and the rim of chronic active lesions (*P*=0.0156). Mann-Whitney test. *n* for each lesion type indicated in **Supplementary Table 1 online**. (d) Representative image of MS lesion with iNOS immunolabeling. Scale bar, 100 μm. (e) Representative image of MS lesion with MR immunolabeling. Scale bar,

100 μm. (f) Co-localization of MR (top) and iNOS (bottom) with microglia/ macrophage marker CD68 (arrowheads). Scale bar, 25 μm. (g) MR+ CD68+ M2 cells (arrows) were sometimes associated with blood vessels. Scale bar, 25 μm.

Figure 8 Activin-A is an M2-derived factor that drives oligodendrocyte differentiation during remyelination.

(a) Percentage of activin-A immunopositive cells per field in M1, M2a, and M2c microglia ± s.e.m. (b) Control corpus callosum lesions at 3 and 10 dpl (top and middle panels) and MCL-injected lesion at 10 dpl (bottom panel) immunostained for activin-A (red) and iNOS or MR (green). Scale bar, 25 μm. (c) Representative images of NG2+ OPCs (green) in remyelinating lesions expressing activin receptors Acvr2A, Acvr2B, and Acvr1B (red; arrows). Scale bar, 10 μm. (d) Percentage of MBP+ cells ± s.e.m. in OPC cultures treated with activin-A. One way ANOVA and Newman-Keuls post-hoc test, *$p<0.05$ (n=4 separate experiments, df=15). (e) Percentage of MBP+ cells ± s.e.m. in OPC cultures treated with combinations of M2a conditioned media, goat isotype control IgG, or goat anti-activin-A antibody. One way ANOVA and Newman-Keuls post-hoc test, **$p<0.01$ (n=4 separate experiments, df=11), ns=$p>0.05$. (f) 300 μm sagittal sections of cerebellum and attached hindbrain were taken from newborn mouse brain to obtain organotypic cultures, demyelinated with lysolecithin (LPC) and treated with M2 conditioned media and either anti-activin-A IgG or control goat IgG. (g) Representative images of slices treated with M2 conditioned media and goat IgG (left) or anti-activin-A antibody (right) immunostained for CC1 (white) and MBP (red). Scale bar, 25 μm. (h) Percentage of CC1+ oligodendrocytes normalized to values obtained from slices treated with IgG alone. 2-tailed one-sample or Student's t-test (respectively), M2 conditioned media +

IgG vs. IgG, *P*=0.0213; M2 conditioned media + IgG vs. M2 conditioned media + anti-activin-A IgG, *P*=0.0071 (*n*=8 slices, df=14). Box plots indicate median (centre line), 25^{th}-75^{th} percentile (box limits), minimum and maximum (whiskers).

Supplemental Material

Supplementary Figure 1 Additional characterization of polarization in corpus callosum lesions.

(a) Representative images of sham PBS-injected lesions at 3 and 10 dpl immunostained for iNOS (green), Arg-1 (red), and CD68 (white). (b) Co-localization of iNOS and Arg-1 in microglia/ macrophage cell bodies (CD68; arrows) and processes (F4/80). 3 and 10 dpl lesions immunostained for additional M1 markers (c; TNFα, CD16/32) and M2 markers (d; MR, IGF-1). All scale bars, 25 μm.

Supplementary Figure 2 Switch from M1- to M2-dominant response in remyelinating lesions of the rat caudal cerebellar peduncle.

(a) Oligodendroglial lineage cell responses following induction of demyelination of the caudal cerebellar peduncle by stereotaxic injection of ethidium bromide (EtBr). Scale bar, 100 μm. (b) Injection of demyelinating toxin induces accumulation of microglia (CD68+; red) at 5 dpl. Recovery of myelin protein expression is observed with re-expression of MAG at 10 dpl (c, centre) and MBP at 21 dpl (c, right). (d) Microglia/ macrophages (CD68+; purple) are present at 5 dpl, increase in abundance at 10 dpl, and decrease in number by 21 dpl. (e) Representative images of lesions immunostained for iNOS (green) and Arg-1 (red). Percentage (f) and mean number (g) of iNOS+ M1, Arg-1+ M2, and unpolarized (iNOS– Arg-1–) cells per field ± s.e.m. at 5, 10, and 21 dpl. One-way ANOVA and Newman-Keuls post test, *$p<0.05$, **$p<0.01$. (n=3, df=26, 17, respectively). (h) 5 and 10 dpl sections immunostained for additional M1 (TNFα, CD16/32) and M2 (IGF-1, MR) markers. All other scale bars, 25 μm.

Supplementary Figure 3 Polarization of cultured microglia to M1 and M2 phenotypes.

(a) Representative images of microglia immunostained against M1 markers iNOS, CD86, CD16/32 (top) and M2 markers MR, Arg-1, and IL1Ra (bottom). Scale bar, 25 μm. (b) Mean percentage of iNOS+ or MR+ cells of total CD68+ cells ± s.e.m.. Kruskal-Wallis test and Dunn's multiple comparison post-hoc test, *p<0.05, **p<0.01, ***p<0.001. (*n*=4) (c) Cropped Western blots showing expression of iNOS with IFNγ/LPS treatment and increase in MR expression with IL-13 or IL-10 treatment, with loading control GAPDH. ELISAs used to assay conditioned media for levels of TNFα (d; *P*=0.0004, *n*=5, df=8), IGF-1 (e; *P*=0.0330, *n*=3, df=4), and IL-10 (f; *P*=0.0051, *n*=5, df=8), presented as mean fold over M0 control ± s.e.m. demonstrating polarization to M1, M2a, and M2c, respectively. A small yet significant increase in IL-10 secretion was observed with IFNγ/ LPS treatment (*P* =0.0081). Polarizing factors alone were included in the assay as a control and did not show detectable levels relative to those measured in conditioned media (d-f). 2-tailed Student's *t*-test.

Supplementary Figure 4 M1 and M2 associated gene expression in cultured microglia.

(a) M1- and M2-associated genes were identified from a previously performed microarray[18] as being significantly upregulated during remyelination of the rat caudal cerebellar peduncles (CCP). These genes were selected for a custom qPCR array to assess gene expression profiles of polarized microglia *in vitro*. (b) Confirmation of expression of additional polarization markers CD86, CCL2, CXCL11, and TGFβ2 in

iNOS+ or Arg-1+ cells in the rat CCP. Scale bar, 5 μm. Microglia treated with IFNγ/LPS (M1), IL13 (M2a), and IL10 (M2c) were analyzed for gene expression levels of (c) *Cd86*, (d) *Cxcl11*, (e) *Ccl2*, (f) *Fcgr2a* (*Cd32*), (g) *Mrc1*(mannose receptor), (h) *Tgfb2*, and (i) *Arg1*, values are represented as $2^{-\Delta Cp}$ ± s.e.m.

Supplementary Figure 5 M1 and M2 microglia conditioned media increase OPC proliferation and migration.

OPCs were treated with microglia conditioned media for 3d. Polarizing factors present in the conditioned media (IFNγ/LPS, IL-13, and IL-10) were directly applied to OPCs as a control. (a) Representative images of OPCs immunostained against NG2 (green) and the proliferative marker Ki67 (red). Double-positive cells are highlighted by arrows. Scale bar, 25 μm. (b) Number of NG2+ cells per field was increased with M0 (*P*=0.005), M1 (*P*=0.00188), M2a (*P*=0.00382), M2c (*P*=0.0119) conditioned media (CM), and IL-10 (*P*=0.0029) compared to control (*n*=5, df=8). (c) Ki67+/NG2+ cells were increased with M0 (*P*=0.0084), M1 (*P*=0.0362), M2a (*P*=0.0194), M2c (*P*=0.0192) conditioned media (*n*=4, df=6) (d) BrdU+ cells were increased with M1 (*P*=0.042), M2a (*P*=0.0083) and M2c conditioned media (*P*=0.0423) (*n*=4, df=6). Values from conditioned media-treated conditions (black bars) and polarizing factors alone (grey bars) were normalized to control (unconditioned media, white bars) in (c) and (d), and are represented as mean ± s.e.m., 2-tailed Student's *t*-test. (e) Number of OPCs ± s.e.m. migrated towards microglia conditioned media (black bars), or polarizing factors alone (grey bars), normalized to values in control (unconditioned media, white bar) showing chemotactic properties of both M1 and M2 conditioned media. Kruskal-Wallis test and Dunn's multiple comparison post-test, **p<0.01, ***p<0.001. (*n*=3).

Supplementary Figure 6 M2 polarized microglia conditioned media promotes the survival of OPCs in a death-inducing environment.

OPCs were treated with microglia conditioned media for 3d in media devoid of serum and growth factors. Polarizing factors present in the conditioned media (IFNγ/LPS, IL-13, and IL-10) were directly applied to OPCs as a control. (a) Representative images of OPCs under basal growth supplemented conditions, grown in deprivation media alone, or supplemented with microglia conditioned media. OPCs were immunostained against NG2 (red) and apoptotic OPCs were visualized by TUNEL assay (green). Scale bar, 50 μm. (b) Mean percentage of TUNEL+ NG2+ OPCs normalized to control supplemented with growth factors and media ± s.e.m.. DNase and ethanol treatment were positive controls for TUNEL positivity. Application of microglia conditioned media to OPCs under normal growth conditions did not induce apoptosis (data not shown). Kruskal-Wallis test and Dunn's multiple comparison post-test, *p<0.05, **p<0.01. (*n*=6).

Supplementary Figure 7 Selective depletion of M1 polarized microglia/ macrophages using gadolinium chloride.

(a) Representative images of M1 (iNOS+; left) and M2a (MR+; right) microglia treated with 270 μm GdCl3 and apoptosis assessed by TUNEL assay (green nuclei). Apoptotic cells are indicated by arrowheads, and were iNOS+ and MR–. Scale bar, 25 μm. (b) Percentage of TUNEL+ M1 microglia treated with vehicle (ctrl), or GdCl3 (0.27-270 μm). Mann-Whitney test, *P*=0.0286. (*n*=4). (c) Mean percentage of TUNEL+ cells ± s.e.m. in M0, M1, M2a, and M2c polarized microglia treated with vehicle or 270 μm GdCl3. One-way ANOVA and Newman-Keuls post-hoc test,

**p<0.01 (*n*=6, df=54). (d) GFAP immunostaining in representative control and GdCl3-injected lesions shows no difference in astrocyte reactivity. Scale bar, 25 μm. (e) Percentage of iNOS+ or Arg-1+ cells in control or GdCl3-injected lesions, *P*=0.0135 (iNOS), 0.0319 (Arg-1), 2-tailed Student's *t*-test (*n*=5, df=8). (f) GdCl3-injected lesions immunostained for M1 markers (iNOS, TNFα, CD16/32) and M2 markers (MR, IGF-1) at 3 dpl. Scale bar, 25 μm. (g) NG2+ (*n*=4, df=6) and Nkx2.2+ (*n*=5, df=8) cells per field in control and GdCl3-treated lesions at 3 dpl. 2-tailed Student's *t*-test, p>0.05. (h) Mean area of MBP and MOG co-localization, fold over control ± s.e.m. in lesions at 21 dpl. *P*=0.081, 2-tailed Student's *t*-test (*n*=6, df=10).

Supplementary Figure 8 Selective depletion of M2 polarized microglia/ macrophages using mannosylated clodronate liposomes.

(a) Representative images of iNOS+ M1 and MR+ M2a microglia treated with MCLs (1:5) and assessed for apoptosis by TUNEL assay. In M1 polarizing conditions, iNOS+ cells were TUNEL– (arrows); TUNEL+ cells were iNOS– (arrowheads). In M2a polarizing conditions, TUNEL+ cells were MR+ (arrowheads), whereas MR– cells were TUNEL– (arrows). (b) Mean percentage of TUNEL+ cells ± s.e.m. in M0, M1, M2a, and M2c polarized microglia treated MCLs (1:5 dilution), normalized to values from M0 conditions. *P*=0.027 (M1 vs. M2a), *P*=0.013 (M1 vs. M2c), 2-tailed Student's *t*-test (*n*=6, df=10). Mean percentage of TUNEL+ cells ± s.e.m. in M2a (c, *P*=0.015, df=7) and M2c (d, *P*=0.0251, 0.0016, 0.03 for 1:50, 1:10, 1:5, respectively, df=6) microglia treated with MCLs (1:200-1:5; black bars) compared to control (white bars) (*n*=4). Mean numbers of microglia per field ± s.e.m. for M2a (e, *P*=0.02, 0.03, 0.009, 0.007 for 1:100, 1:50, 1:10, 1:5, respectively, df=6) and M2c (f; *P*=0.0003, <0.0001, 0.0005, 0.0005 for 1:100, 1:50, 1:10, 1:5, respectively, df=6)

polarized cells treated with MCLs (1:200-1:5; black bars) compared to control (white bars), 2-tailed Student's *t*-test (*n*=4). (g) Percentage of iNOS+ M1, Arg-1+ M2, or unpolarized (iNOS–, Arg-1–) cells per field ± s.e.m. in control and MCL-injected lesions at 10 dpl. *P*<0.0001, 2-tailed Student's *t*-test (*n*=5, df=8). (h) MCL-injected lesions immunostained for additional M1 (iNOS, TNFα, CD16/32) and M2 markers (MR, IGF-1). Scale bar, 25 μm. (i) Mean area of MBP and MOG colocalization fold over control ± s.e.m. in lesions at 21 dpl. 2-tailed Student's *t*-test, *P*=0.0002 (*n*=6, df=10). (j) Axons (NF+) were detectable running through the lesion (MBP–) at 10 dpl following MCL injection. (k) MCL injection did not influence astrocytes (GFAP+) within the lesion. Scale bar, 25 μm. (l) Total numbers of Nkx2.2+ OPCs ± s.e.m. in control and MCL injected lesions. 2-tailed Student's *t*-test, p>0.05 (*n*=4, df=6).

Supplementary Figure 9 Expression of activin-A receptors on cells in remyelinating lesions.

Representative images of oligodendrocytes (CC1+), microglia/ macrophages (CD68+), astrocytes (GFAP+), and neurons (axons; NF+) with expression, or lack thereof, of activin-A receptors Acvr2A and Acvr2B. Scale bar, 10 μm.

Supplemental Table 1. Human brain tissue samples

	Classification	Sex	Age	Disease duration (yrs)	Block	Lesions Analyzed			
						Active	Chronic Active	Chronic Inactive	Remyelinated
Multiple Sclerosis Patients	SPMS	M	46	8	P2E3	0	0	2	2
					P3E3	1	0	1	1
	SPMS	F	49	14	A3D3	3	0	0	0
	SPMS	M	40	9	P3B4	1	0	1	3
	SPMS	F	60	21	P3C3	1	1	1	0
	SPMS	F	34	21	A2D7	1	0	0	0
					A2E2	1	0	1	1
	PPMS	M	37	27	P4D1	0	0	1	3
	SPMS	F	57	27	P3D1	0	0	0	2
	SPMS	F	46	25	A2B3	0	1	1	0
					P2C4	0	2	0	1
	SPMS	F	42	19	A2C2	2	0	0	1
	SPMS	F	57	19	P3C4	0	2	3	0
					TOTAL	**10**	**6**	**11**	**14**
Non-Neurological Controls	Carcinoma of the lung metastasized	M	77	-	P3B4	-	-	-	-
	Cardiac failure	M	64	-	P2D2	-	-	-	-
	Carcinoma of the tongue	M	35	-	P3B3	-	-	-	-
	Ovarian cancer	F	60	-	P3D2	-	-	-	-
	Myelodysplastic syndrome, Rheumatoid Arthritis	M	82	-	A2C7	-	-	-	-

ONLINE METHODS

In vivo focal CNS white matter demyelinating lesions and parabiosis.

Demyelinating lesions were induced in the corpus callosum of 10-17 week-old male C57BL/6 mice or the caudal cerebellar peduncles of 12 week-old female Sprague Dawley rats by stereotaxic injection of 2 µl of 1% lysolecithin (v/v) or 4 µl of 0.01% ethidium bromide (v/v), respectively, using a Hamilton syringe. Sham lesions were induced by phosphate buffered saline (PBS) injection. Lesions were also induced in the corpus callosum of 10 week-old male CCR2 null mice (B6.129S4-*Ccr2*^{tm1lfc}/J; The Jackson Laboratory). A subset of these underwent tail vein injections of 5x10^6 bone marrow cells derived from GFP mice of the same age/ sex (C57BL/6-Tg(CAG-EGFP)131Osb/LeySopJ;The Jackson Laboratory) 1 day prior to lesioning (for 3 day time points) or 8 days post lesion (for 10 day time points). Animals were intracardially perfused with 4% paraformaldehyde (PFA), and brains were post-fixed overnight and cryoprotected in sucrose prior to OCT embedding (Tissue-Tech) and storage at -80°C. All experiments were performed under the UK Home Office project licences issued under the Animals (Scientific Procedures) Act. C57BL/6 isogenic or congenic female mice were joined by parabiosis as previously described [4]. Isochronic parabiosis involved young-young pairs (5-7 weeks old) and old-old pairs (10-12 months old), whereas heterochronic parabiosis involved young-old pairs (young partner was wildtype or GFP-expressing (C57BL/6-UBC-GFP; Jackson Laboratories)). Demyelinated lesions were induced in the ventral funiculus of the thoracic column of the spinal cord by injection of 1% lysolecithin [4] and animals perfused as above. These experiments were carried out at the Joslin Diabetes Centre animal facility (Boston, MA) and the BRI animal facility in the Department of Stem Cell and Regenerative Biology (Harvard University, Cambridge, MA) in compliance

with guidelines from the Institutional Animal Care and Use Committee (IACUC) of Joslin Diabetes Centre and Harvard University.

Selective depletion of M1 or M2 microglia in focal demyelinated lesions. GdCl3 (Sigma; 0.27-1000 μM) was applied to microglia *in vitro* during polarization to assess its specificity in inducing apoptosis in M1 phenotypes by terminal deoxynucleotidyl transferase dUTP nick end labelling (TUNEL) assay. PBS or GdCl3 (270 μM) was stereotaxically co-injected into the corpus callosum of mice with lysolecithin and depletion of M1 microglia/ macrophages was assessed at 3dpl. Mannosylated clodronate (dichloromethylene diphosphonate; Cl_2MDP)-encapsulated liposomes (Encapsula Nano Sciences) were applied to polarized microglia *in vitro* diluted in culture media (1:5-1:200) to assess specificity in promoting M2 apoptosis by TUNEL assay. PBS or undiluted clodronate liposomes were stereotaxically injected into the lesion site at 8 dpl and depletion of M2 microglia/ macrophages was assessed at 10 dpl.

Immunohistochemistry. Slides were air-dried, permeabilized, and blocked for 1h and primary antibody applied overnight at 4°C in a humid chamber. Fluorescently-conjugated secondary antibodies were applied for 2 h at room temperature in a humid chamber (1:500, Molecular Probes and Jackson ImmunoResearch). Biotin-conjugated isolectin B4 (1:100, Sigma Aldrich L-2140) was labelled with avidin-Alexa 488 (1:500, Molecular Probes). Following counterstaining with Hoechst, slides were coverslipped with Fluoromount-G (Southern Biotech). Antibody isotype controls (Sigma) added to sections at the same final concentration as the respective primary antibodies showed little or no non-specific staining. Antibodies used to detect M1

microglia/ macrophage markers are as follows: mouse anti-iNOS (BD Biosciences, 610329, 1:100), rat anti-CD16/32 (BD Pharmingen, 553141/2, 1:500), goat anti-TNFα (R&D Systems, AB-410-NA, 1:500), rabbit anti-CD86 (Abcam, ab53004, 1:100), rabbit anti-CCL2 (Biorbyt, orb36895, 1:100), and rabbit anti-CXCL11 (Biorbyt, orb33040, 1:100). Antibodies used to detect M2 markers are as follows: goat anti-Arginase-1 (Santa Cruz Biotechnology, sc-18355, 1:50), rabbit anti-mannose receptor (Abcam, ab64693, 1:600), goat anti-IGF-1 (R&D Systems, AF791, 1:100), rabbit anti IL1Ra (Santa Cruz Biotechnology, sc-25444, 1:100), and goat anti-pan TGFβ (R&D Systems, AB-100-NA,1:500). Antibodies used against pan microglia/ macrophage markers include rat anti-CD68 (Abcam, ab53444, 1:100) and rat anti-F4/80 (Abcam, ab6640, 1:100). Oligodendrocyte and myelin antigens were detected by rabbit or mouse anti-NG2 (Millipore, MAB5384/ 5320, 1:200, 1:100, respectively), mouse anti-Nkx2.2 (Developmental Hybridoma Bank, clone 74.5A5-c, University of Iowa, 1:100), mouse anti-CC1 (Abcam, ab16794, 1:100), rat anti-MBP (AbD Serotec, MCA409S, 1:250), rabbit anti-damaged MBP (Millipore, AB5864, 1:100), and mouse anti-MOG and anti-MAG (Millipore, MAB5680/ 1567, 1:100). Antibodies to detect nodes of Ranvier include rabbit anti-Caspr (Abcam, ab34151, 1:500) and mouse anti-Ankyrin-G (UC Davis/ NIH NeuroMab Facility, clone N106/36, 1:200). Antibodies against activin-A or its receptors include goat anti-activin-A (AF338), anti-Acvr1B (AF1477), anti-Acvr2A (AF340), and anti-Acvr2B (AF339) (all from R&D Systems, 1:40). Other antibodies include chicken anti-NFH (Encor Biotechnology, Inc., CPCA-NF-H, 1:10,000), rabbit anti-GFAP (DAKO, Z0334, 1:500), rabbit anti-Ki67 (Abcam, AB9620, 1:100), rabbit anti-PCNA (Abcam, ab2426-1, 1:100), and chicken anti-GFP (Abcam, ab13970, 1:100).

Microglia and OPC Culture. Cortical mixed glial cultures were generated from Sprague Dawley rat postnatal day 0-2 pups. Microglia were isolated by collecting the floating fraction of 10 day-old mixed glial cultures following 1 hr on a rotary shaker at 37°C at 250 rpm, and plated in Dulbecco's modified essential media (DMEM) containing 4.5 g/L glucose, L-glutamine, pyruvate, 10% fetal calf serum, and 1% penicillin/streptomycin ('DMEM 10%'; GIBCO) on poly-D-lysine (PDL)-coated 16-well glass chamberslides (Lab-TEK) at $5x10^4$ cells/well, or at $1x10^6$ cells/ well on PDL-coated glass coverslips in a 24 well plate. For survival experiments, microglia were grown in serum-free media to avoid confounding pro-survival effects of serum in the conditioned media; successful polarization under these growth conditions was confirmed (data not shown). OPCs were isolated by collecting the floating fraction of 10 day-old mixed glial cultures following depletion of microglia as above, 16 hr on a rotary shaker at 37°C at 250 rpm, and depletion of astrocytes by differential adhesion. OPCs were plated in DMEM containing 4.5 g/L glucose, L-glutamine, pyruvate, SATO (16 μg/ml putrescine, 400 ng/ml L-thyroxine, 400 ng/ml tri-iodothyroxine, 60 ng/ml progesterone, 5 ng/ml sodium selenite, 100 μg/ml bovine serum albumin fraction V, 10 μg/ml insulin, 5.5 μg/ml halo-transferrin (all from Sigma-Aldrich)), 0.5% fetal calf serum (GIBCO), 1% penicillin/streptomycin, 10 ng/ml platelet-derived growth factor, and 10 ng/ml fibroblast growth factor-2 at $2x10^4$ cells per well in PDL-coated plastic chamberslides (Lab-TEK). OPCs were treated for 3 days with microglia media as a control or conditioned media added in a 1:1 ratio to OPC culture media. 5-bromo-2'-deoxyuridine (BrdU) was added to OPC cultures for 24 h prior to fixation. Activin-A (1-100 ng/ml; R&D Systems) or vehicle (0.1% BSA in PBS) was added to OPCs for 3 days. Goat anti-activin-A (βA subunit) blocking antibody (200 ng/ml; R&D Systems) or goat IgG control (200 ng/ml; Santa Cruz Biotechnology, Inc.)

diluted in OPC culture media was added to cultures with M2a conditioned media in a 1:1 ratio for 3 days. All assays represent a minimum of 3 independent experiments treated with conditioned media from at least 3 microglial preparations. 2-4 20X or 40X objective images were taken per condition per experiment for quantification.

Microglia polarization. Microglia were either left untreated or treated overnight with IFNγ (20 ng/ml) and LPS (0127:B8, 100 ng/ml), IL-13 (50ng/ml), or IL-10 (10ng/ml) (all from Sigma-Aldrich; <1 EU/μg). Conditioned media was collected and stored at -20°C. Contaminating astrocytes were < 7% of the culture in all polarization states (data not shown). ELISAs for TNFα, IGF-1, and IL-10 were used according to the manufacturer's instructions (R&D Systems). Absorbance was read at 450nm on a spectrophotometer and sample concentrations calculated using an equation generated from a standard curve. 3-5 independent supernatant sets were used. The rapid depolarization of microglia in the absence of polarizing factors (data not shown) required these to be present during conditioning of media; polarizing factors alone were directly applied to OPCs as a control.

Protein extraction & Western blotting. Lysates were generated using RIPA buffer (Thermo Scientific) supplemented with 1% protease inhibitor cocktail set III ethylenediaminetetraaceticacid (EDTA)-free (Calbiochem). Protein concentrations were determined using the Pierce BCA Protein Assay Kit according to the manufacturer's instructions. Samples were diluted in Laemmli buffer [200mM Tris-HCl pH6.8 (Sigma-Aldrich), 8% sodium dodecyl sulphate (Sigma-Aldrich), 40% glycerol (BioRad), 0.2% bromophenol blue (Sigma) and 5% β-mercaptoethanol (Sigma)], heated at 95ºC for 2 min, and 10 μg of protein was loaded onto an

acrylamide gel (4-20%; Thermo Scientific). Gel electrophoresis was performed in Tris-hydroxyethyl piperazineethanesulfonic acid (HEPES)-sodium dodecyl sulphate (SDS) running buffer (Thermo Scientific) at 150 V for 45 minutes and proteins transferred onto polyvinylidene difluoride (PVDF) membranes (Millipore) for 2h at 400 mA in 10% transfer buffer [3% Tris-HCl (Sigma-Aldrich), 15% glycine (Sigma-Aldrich), pH 8.3] and 20% methanol (Fisher Chemical) diluted in H_2O. Membranes were blocked with 5% powdered milk (<1% fat) in Tris-buffered saline (TBST) [4% sodium chloride (NaCl), 0.1% potassium chloride (KCl), 1.5% Tris-HCl, 0.1% Tween-20 (all from Sigma-Aldrich), pH 7.4] for 1 h at room temperature on an orbital shaker, and incubated overnight at 4ºC with mouse anti-iNOS (1:500; BD Bioscience) or rabbit anti-MR antibody (1:500; Abcam), washed thrice in TBST for 5 min, and incubated with horseradish peroxidase (HRP)-IgG secondary antibody conjugates (1:10,000; Calbiochem) for 1 h at room temperature. Chemiluminescent substrate detection reagent RapidStep ECL Reagent (Calbiochem) and autoradiography film processing was performed. For loading control purposes, all membranes were re-blotted with anti-mouse (1:1000, Millipore) or anti-rabbit glyceraldehyde-3-phosphate dehydrogenase antibody (GAPDH; 1:1000, Sigma).

Transfilter microchemotaxis assays. OPCs were plated on PDL-coated poly-carbonate transwell culture inserts (Corning) in a 24 well plate at $5x10^4$ cells/ well in basal culture media supplemented with fibroblast growth factor (FGF2). Platelet derived growth factor (PDGF) was excluded from the media due to its chemoattractant properties. Microglia media, conditioned media, or recombinant polarization factors were added to the bottom chamber in a 1:1 ratio with OPC culture media. Cells were allowed to migrate for <24 hrs at 37°C to avoid confounding

effects of conditioned media on proliferation. Cells were fixed for 1h with 4% PFA and 0.1% glutaraldehyde. Unmigrated cells on the upper side of the transwell were scraped off with a cotton swab, and cells that had migrated to the bottom of the transwell were visualized with Hoechst. Each condition was performed in quadruplicate wells and the experiment was repeated with 3 independent OPC samples and 3 conditioned media samples. 4 images were taken per well at 20X magnification for quantification purposes.

Immunocytochemistry. Cells were fixed with 4% paraformaldehyde (Sigma) for 10-15 min and blocked for 30 minutes at room temperature. Primary antibodies were diluted in blocking solution and applied for 1 h at room temperature (as listed above). Cells were incubated with fluorescently conjugated secondary antibodies (1:1000, Invitrogen) for 1 h at room temperature, counterstained with Hoechst (5 μg/ml), and coverslipped with fluoromount-G. Apoptotic cells were visualized by TUNEL assay (Promega) according to the manufacturer's instructions. Positive controls for apoptosis included addition of 70% ethanol to live cells, and incubation of fixed cells with DNase (10 units/ml) for 10 min. For proliferation studies, BrdU-treated OPCs were fixed with ice-cold 70% ethanol in 50 mM glycine buffer, pH 2.0, for 20 minutes. Permeabilization was performed with 2M HCl for 15 min at 37°C, which was neutralized by 3 washes in TBE buffer (1M Tris, 0.9M Boric acid, 0.01M EDTA; GIBCO).

RNA extraction, reverse transcription, and quantitative real-time polymerase chain reaction array (qRT-PCR). Microglia were washed with PBS, lysed with RLT buffer supplemented with beta-mercaptoethanol, scraped, and homogenized with

21 guage needles. RNA extraction was performed using the Qiagen minikit (with on-column DNase treatment), and reverse transcription performed using the Invitrogen Superscipt First-strand synthesis system for RT-PCR, both according to the manufacturer's instructions. A custom qPCR array plate (SABiosciences) was designed to include primers for M1 and M2-associated genes that were detected as being significantly upregulated in a microarray screen of a remyelinating lesion of the rat caudal cerebellar peduncles *in vivo* [18]. qPCR was carried out using the Roche Light Cycler 480. Cp values were obtained using the second derivative maximum method and ΔCp was calculated by subtracting the average value from 5 housekeeping genes (*Actb*, *B2m*, *Ldha*, *Pgk1*, *Hprt1*). Expression is represented as $2^{-\Delta Cp}$.

Organotypic cerebellar slice cultures. Cerebellum and attached hindbrain were isolated from P0-P2 CD1 mouse pups, sectioned sagitally at 300 μm on McIlwain tissue chopper, and plated onto Millipore-Millicel-CM mesh inserts (Fisher Scientific) in 6 well culture plates at 6 slices per insert. Media was composed of 50% minimal essential media, 25% heat-inactivated horse serum, 25% Earle's balanced salt solution (all from GIBCO), 6.5 mg/ml glucose (Sigma), 1% penicillin-streptomycin, and 1% glutamax, and was changed every 2-3 days. Demyelination was induced at 21 days in vitro (DIV) by a 20 hr incubation in 0.5 mg/ml lysolecithin, slices were washed in media for 10 min. After recovery, slices were treated for 6 days with M2a microglia conditioned media and either anti-activin-A goat IgG or isotype control (200 ng/ml). Slices were fixed in 4% PFA for 1 hr. Primary antibody (as listed above) was applied for 48 hr at 4°C, slices were washed thrice, and fluorescently conjugated antibody was applied overnight at 4°C. Slices were mounted onto glass slides using Fluoromount-G.

Multiple Sclerosis Tissue. Post-mortem tissue from MS patients and controls that died of non-neurological causes were obtained via a UK prospective donor scheme with full ethical approval from the UK Multiple Sclerosis Tissue Bank (MREC/02/2/39). Diagnosis of MS was confirmed by neuropathological means by Dr F. Roncaroli (Consultant Neuropathologist, Imperial College London) and clinical history was provided by Dr R. Nicholas (Consultant Neurologist, Imperial College London) (summarized in **Supplementary Table 1 online**). The death-to-tissue preservation interval was from 7-31 h. Brain blocks numbered by the brain bank locate the position of the block in the brain (i.e. coronal plane: anterior (A) and posterior (P) halves at the mamillary bodies, and 1 cm coronal slices numbered sequentially, vertical plane: 2×2 cm blocks identified by letters (A–E) and by numbers in the horizontal plane). Snap frozen unfixed tissue blocks (2×2×1 cm) were cut at 10 μm and stored at −80°C. MS lesions were classified according to the International Classification of Neurological Disease using luxol fast blue staining and CD68+ immunoreactivity. We analysed 5 control blocks and 13 tissue blocks from 10 MS patients; in total, we analysed 10 active lesions, 6 chronic active lesions, 11 chronic inactive lesions, and 14 remyelinated lesions (**Supplementary Table 1 online**). Approximately 170 fields of 50 μm x 50 μm were counted per lesion and counts were multiplied to determine density of immunopositive cells/ mm^2. Sections were fixed in 4% PFA for 1 h at room temperature, washed in PBS, and permeabilized in methanol for 10 min at -20°C. Following washes in 0.3% Triton X-100 in PBS, sections were microwaved in Vector unmasking solution for 10 min, and endogenous peroxidase activity blocked for 5 min (Envision blocking solution, DAKO). Primary antibody was prepared in antibody diluent (AMS Biotechnology (Europe) Ltd) and applied

overnight in a humid chamber at 4°C. Antibodies used include mouse anti-iNOS (BD Bioscience, 610329, 1:100), rabbit anti-mannose receptor (Abcam, ab64693, 1:600), and mouse anti-CD68 (DAKO, clone KP1 M0814, 1:100). Following 3 washes in 0.3% Triton X-100 in PBS, anti-mouse or –rabbit peroxidase conjugated secondary antibody was applied for 2h at room temperature in a humid chamber. Sections were washed in PBS and stains visualized by 3,3'-Diaminobenzidine (DAB) chromagen. Following washes in water, sections were dehydrated in increasing concentrations of acetone, then xylene, and coverslipped. For co-localization stains, sections were blocked with 10% normal horse serum and 0.1% Triton-X 100 for 1h, antibodies applied overnight as above, and fluorescently conjugated secondary antibodies (Invitrogen) applied for 2h with Hoechst counterstain.

Quantification and statistical analysis. Lesion pixel counts and area quantification for MAG and MBP expression were performed using 10X objective images thresholded using Image J (NIH). The area of MOG and MBP co-localization in 40X objective images was obtained with Image J using the RG2B Colocalization Plugin followed by area quantification. All manual cell counts were performed in a blinded manner. Data are represented as mean ± s.e.m.. No statistical methods were used to predetermine sample sizes but these were similar to those generally employed in the field. Data was first tested for normality using the Kolmogorov-Smirnov test. Multiple comparisons within the same data set were analyzed by one-way ANOVA with Newman-Keuls post-hoc test, or Kruskal-Wallis test and Dunn's multiple comparison test. Single comparisons to control were made using 2-tailed Student's *t*-test or Mann-Whitney test. *P* values of <0.05 were considered statistically significant.

Data handling and statistical processing was performed using Microsoft Excel and GraphPad Prism Software.

REFERENCES

1. Banati,R.B., Gehrmann,J., Schubert,P., & Kreutzberg,G.W. Cytotoxicity of microglia. *Glia* **7**, 111-118 (1993).

2. Cash,E., Zhang,Y., & Rott,O. Microglia present myelin antigens to T cells after phagocytosis of oligodendrocytes. *Cell Immunol.* **147**, 129-138 (1993).

3. Kotter,M.R., Li,W.W., Zhao,C., & Franklin,R.J. Myelin impairs CNS remyelination by inhibiting oligodendrocyte precursor cell differentiation. *J. Neurosci.* **26**, 328-332 (2006).

4. Ruckh,J.M. *et al.* Rejuvenation of regeneration in the aging central nervous system. *Cell Stem Cell* **10**, 96-103 (2012).

5. Kotter,M.R., Zhao,C., van,R.N., & Franklin,R.J. Macrophage-depletion induced impairment of experimental CNS remyelination is associated with a reduced oligodendrocyte progenitor cell response and altered growth factor expression. *Neurobiol. Dis.* **18**, 166-175 (2005).

6. Ruffell,D. *et al.* A CREB-C/EBPbeta cascade induces M2 macrophage-specific gene expression and promotes muscle injury repair. *Proc. Natl. Acad. Sci. U. S. A* **106**, 17475-17480 (2009).

7. Dayan,V. *et al.* Mesenchymal stromal cells mediate a switch to alternatively activated monocytes/macrophages after acute myocardial infarction. *Basic Res. Cardiol.* **106**, 1299-1310 (2011).

8. Deonarine,K. *et al.* Gene expression profiling of cutaneous wound healing. *J. Transl. Med.* **5**, 11 (2007).

9. Edwards,J.P., Zhang,X., Frauwirth,K.A., & Mosser,D.M. Biochemical and functional characterization of three activated macrophage populations. *J. Leukoc. Biol.* **80**, 1298-1307 (2006).

10. Gensert,J.M. & Goldman,J.E. Endogenous progenitors remyelinate demyelinated axons in the adult CNS. *Neuron* **19**, 197-203 (1997).

11. Nait-Oumesmar,B. *et al.* Progenitor cells of the adult mouse subventricular zone proliferate, migrate and differentiate into oligodendrocytes after demyelination. *Eur. J. Neurosci.* **11**, 4357-4366 (1999).

12. Arnett,H.A. *et al.* bHLH transcription factor Olig1 is required to repair demyelinated lesions in the CNS. *Science* **306**, 2111-2115 (2004).

13. Etxeberria,A., Mangin,J.M., Aguirre,A., & Gallo,V. Adult-born SVZ progenitors receive transient synapses during remyelination in corpus callosum. *Nat. Neurosci.* **13**, 287-289 (2010).

14. Woodruff,R.H. & Franklin,R.J. The expression of myelin protein mRNAs during remyelination of lysolecithin-induced demyelination. *Neuropathol. Appl. Neurobiol.* **25**, 226-235 (1999).

15. Ajami,B., Bennett,J.L., Krieger,C., McNagny,K.M., & Rossi,F.M. Infiltrating monocytes trigger EAE progression, but do not contribute to the resident microglia pool. *Nat. Neurosci.* **14**, 1142-1149 (2011).

16. Voss,E.V. *et al.* Characterisation of microglia during de- and remyelination: can they create a repair promoting environment? *Neurobiol. Dis.* **45**, 519-528 (2012).

17. Saederup,N. *et al.* Selective chemokine receptor usage by central nervous system myeloid cells in CCR2-red fluorescent protein knock-in mice. *PLoS. One.* **5**, e13693 (2010).

18. Huang,J.K. *et al.* Retinoid X receptor gamma signaling accelerates CNS remyelination. *Nat. Neurosci.* **14**, 45-53 (2011).

19. Pendino,K.J., Meidhof,T.M., Heck,D.E., Laskin,J.D., & Laskin,D.L. Inhibition of macrophages with gadolinium chloride abrogates ozone-induced pulmonary injury and inflammatory mediator production. *Am. J. Respir. Cell Mol. Biol.* **13**, 125-132 (1995).

20. Abdel-Zaher,A.O., Abdel-Rahman,M.M., Hafez,M.M., & Omran,F.M. Role of nitric oxide and reduced glutathione in the protective effects of aminoguanidine, gadolinium chloride and oleanolic acid against acetaminophen-induced hepatic and renal damage. *Toxicology* **234**, 124-134 (2007).

21. Mizgerd,J.P., Molina,R.M., Stearns,R.C., Brain,J.D., & Warner,A.E. Gadolinium induces macrophage apoptosis. *J. Leukoc. Biol.* **59**, 189-195 (1996).

22. Hardonk,M.J., Dijkhuis,F.W., Hulstaert,C.E., & Koudstaal,J. Heterogeneity of rat liver and spleen macrophages in gadolinium chloride-induced elimination and repopulation. *J. Leukoc. Biol.* **52**, 296-302 (1992).

23. Marin-Teva,J.L. *et al.* Microglia promote the death of developing Purkinje cells. *Neuron* **41**, 535-547 (2004).

24. Serrats,J. *et al.* Dual roles for perivascular macrophages in immune-to-brain signaling. *Neuron* **65**, 94-106 (2010).

25. Das,J. *et al.* A critical role for NF-kappa B in GATA3 expression and TH2 differentiation in allergic airway inflammation. *Nat. Immunol.* **2**, 45-50 (2001).

26. Jang,E. *et al.* Secreted protein lipocalin-2 promotes microglial M1 polarization. *FASEB J.*(2012).

27. Fancy,S.P. *et al.* Axin2 as regulatory and therapeutic target in newborn brain injury and remyelination. *Nat. Neurosci.* **14**, 1009-1016 (2011).

28. Yuen,T.J. *et al.* Identification of endothelin 2 as an inflammatory factor that promotes central nervous system remyelination. *Brain* **136**, 1035-1047 (2013).

29. He,J.T. *et al.* Neuroprotective effects of exogenous activin A on oxygen-glucose deprivation in PC12 cells. *Molecules.* **17**, 315-327 (2012).

30. Sakai,T. & Xu,Y. Stem cells decreased neuronal cell death after hypoxic stress in primary fetal rat neurons in vitro. *Cell Transplant.* **21**, 355-364 (2012).

31. de Kretser,D.M., O'Hehir,R.E., Hardy,C.L., & Hedger,M.P. The roles of activin A and its binding protein, follistatin, in inflammation and tissue repair. *Mol. Cell Endocrinol.* **359**, 101-106 (2012).

32. Ahn,M. *et al.* Immunohistochemical study of arginase-1 in the spinal cords of Lewis rats with experimental autoimmune encephalomyelitis. *Brain Res.* **1453**, 77-86 (2012).

33. Attisano,L., Wrana,J.L., Montalvo,E., & Massague,J. Activation of signalling by the activin receptor complex. *Mol. Cell Biol.* **16**, 1066-1073 (1996).

34. Matzuk,M.M., Kumar,T.R., & Bradley,A. Different phenotypes for mice deficient in either activins or activin receptor type II. *Nature* **374**, 356-360 (1995).

35. Matzuk,M.M. Functional analysis of mammalian members of the transforming growth factor-beta superfamily. *Trends Endocrinol. Metab* **6**, 120-127 (1995).

36. Mikita,J. *et al.* Altered M1/M2 activation patterns of monocytes in severe relapsing experimental rat model of multiple sclerosis. Amelioration of clinical status by M2 activated monocyte administration. *Mult. Scler.* **17**, 2-15 (2011).

37. Olah,M. *et al.* Identification of a microglia phenotype supportive of remyelination. *Glia* **60**, 306-321 (2012).

38. Liang,X., Draghi,N.A., & Resh,M.D. Signaling from integrins to Fyn to Rho family GTPases regulates morphologic differentiation of oligodendrocytes. *J. Neurosci.* **24**, 7140-7149 (2004).

39. Thurnherr,T. *et al.* Cdc42 and Rac1 signaling are both required for and act synergistically in the correct formation of myelin sheaths in the CNS. *J. Neurosci.* **26**, 10110-10119 (2006).

40. Flores,A.I. *et al.* Constitutively active Akt induces enhanced myelination in the CNS. *J. Neurosci.* **28**, 7174-7183 (2008).

41. Guardiola-Diaz,H.M., Ishii,A., & Bansal,R. Erk1/2 MAPK and mTOR signaling sequentially regulates progression through distinct stages of oligodendrocyte differentiation. *Glia* **60**, 476-486 (2012).

42. Diemel,L.T., Jackson,S.J., & Cuzner,M.L. Role for TGF-beta1, FGF-2 and PDGF-AA in a myelination of CNS aggregate cultures enriched with macrophages. *J. Neurosci. Res.* **74**, 858-867 (2003).

43. McKinnon,R.D., Piras,G., Ida,J.A., Jr., & Dubois-Dalcq,M. A role for TGF-beta in oligodendrocyte differentiation. *J. Cell Biol.* **121**, 1397-1407 (1993).

44. Kigerl,K.A. *et al.* Identification of two distinct macrophage subsets with divergent effects causing either neurotoxicity or regeneration in the injured mouse spinal cord. *J. Neurosci.* **29**, 13435-13444 (2009).

45. Liao,B., Zhao,W., Beers,D.R., Henkel,J.S., & Appel,S.H. Transformation from a neuroprotective to a neurotoxic microglial phenotype in a mouse model of ALS. *Exp. Neurol.* **237**, 147-152 (2012).

46. Kuhlmann,T. *et al.* Differentiation block of oligodendroglial progenitor cells as a cause for remyelination failure in chronic multiple sclerosis. *Brain* **131**, 1749-1758 (2008).

47. Schaier,M. *et al.* Role of FTY720 on M1 and M2 macrophages, lymphocytes, and chemokines in 5/6 nephrectomized rats. *Am. J. Physiol Renal Physiol* **297**, F769-F780 (2009).

48. Weber,M.S. *et al.* Type II monocytes modulate T cell-mediated central nervous system autoimmune disease. *Nat. Med.* **13**, 935-943 (2007).

Nature Neuroscience 16, 1211–1218 (2013) doi:10.1038/nn.3469

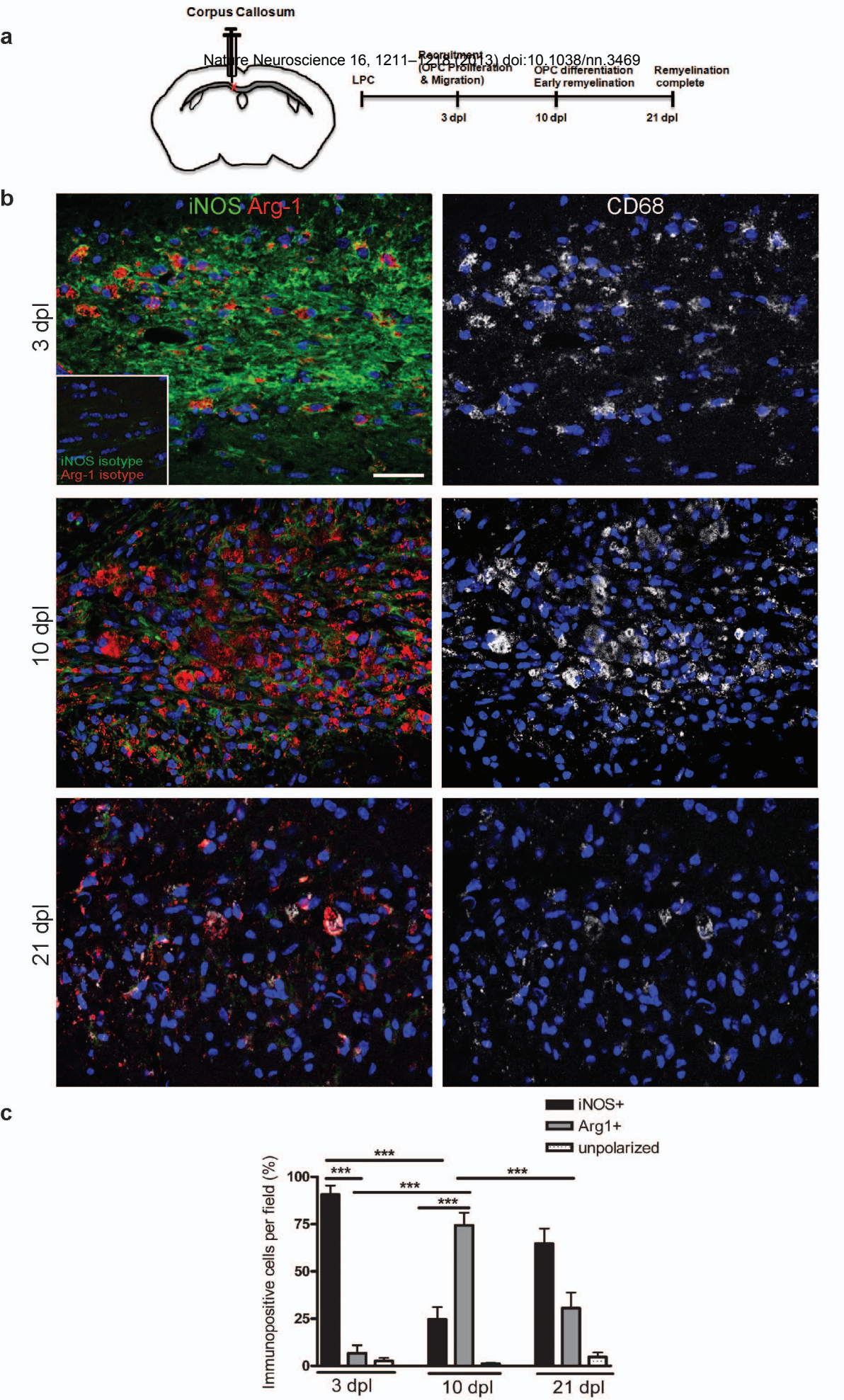

Nature Neuroscience 16, 1211–1218 (2013) doi:10.1038/nn.3469

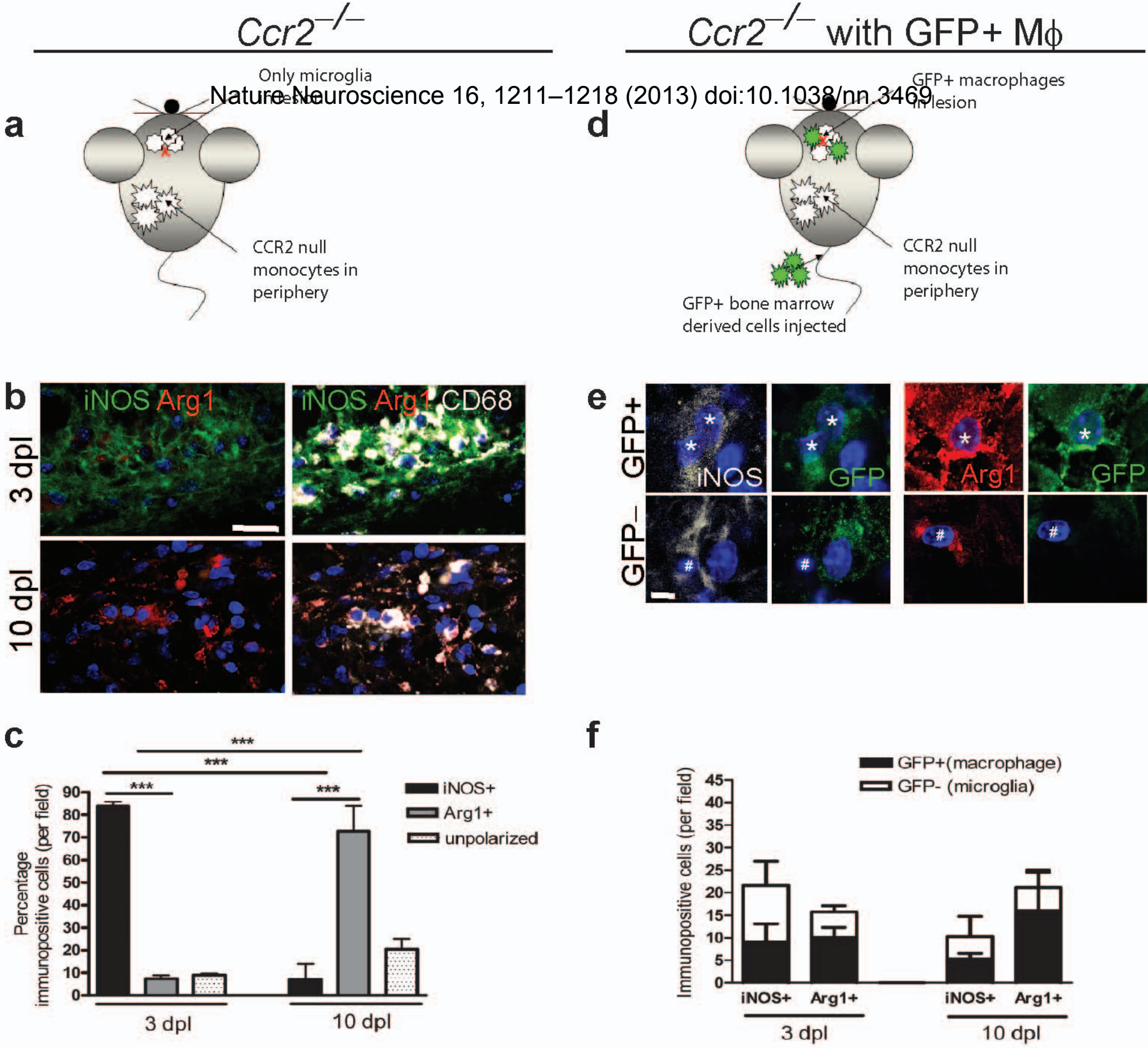

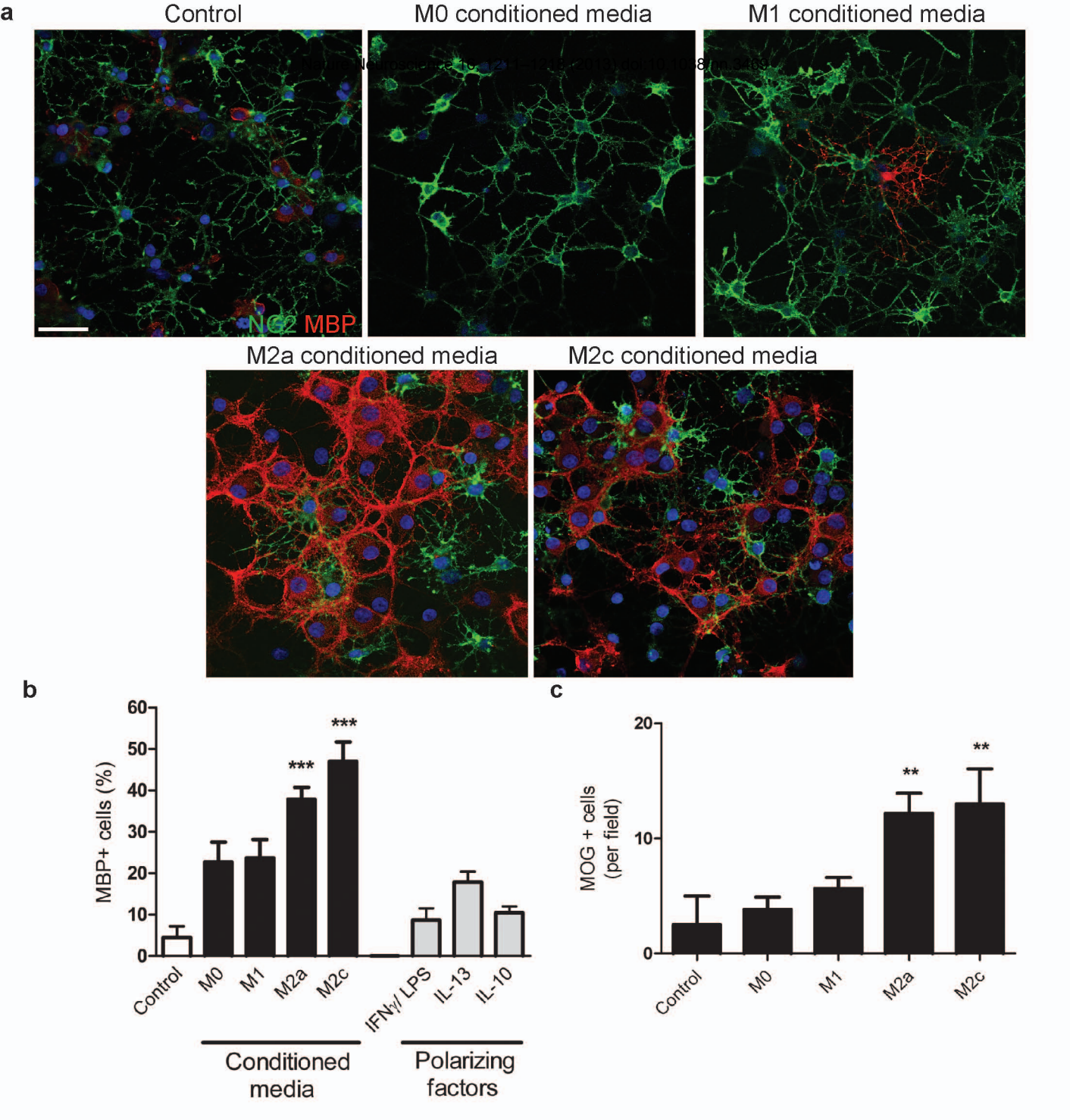
a
Control
M0 conditioned media
M1 conditioned media
NG2 MBP
M2a conditioned media
M2c conditioned media
b
MBP+ cells (%)
60
50
40
30
20
10
0
***
***
Control
M0
M1
M2a
M2c
IFNγ/ LPS
IL-13
IL-10
Conditioned media
Polarizing factors
c
MOG + cells (per field)
20
10
0
**
**
Control
M0
M1
M2a
M2c

Nature Neuroscience 16, 1211–1218 (2013) doi:10.1038/nn.3469

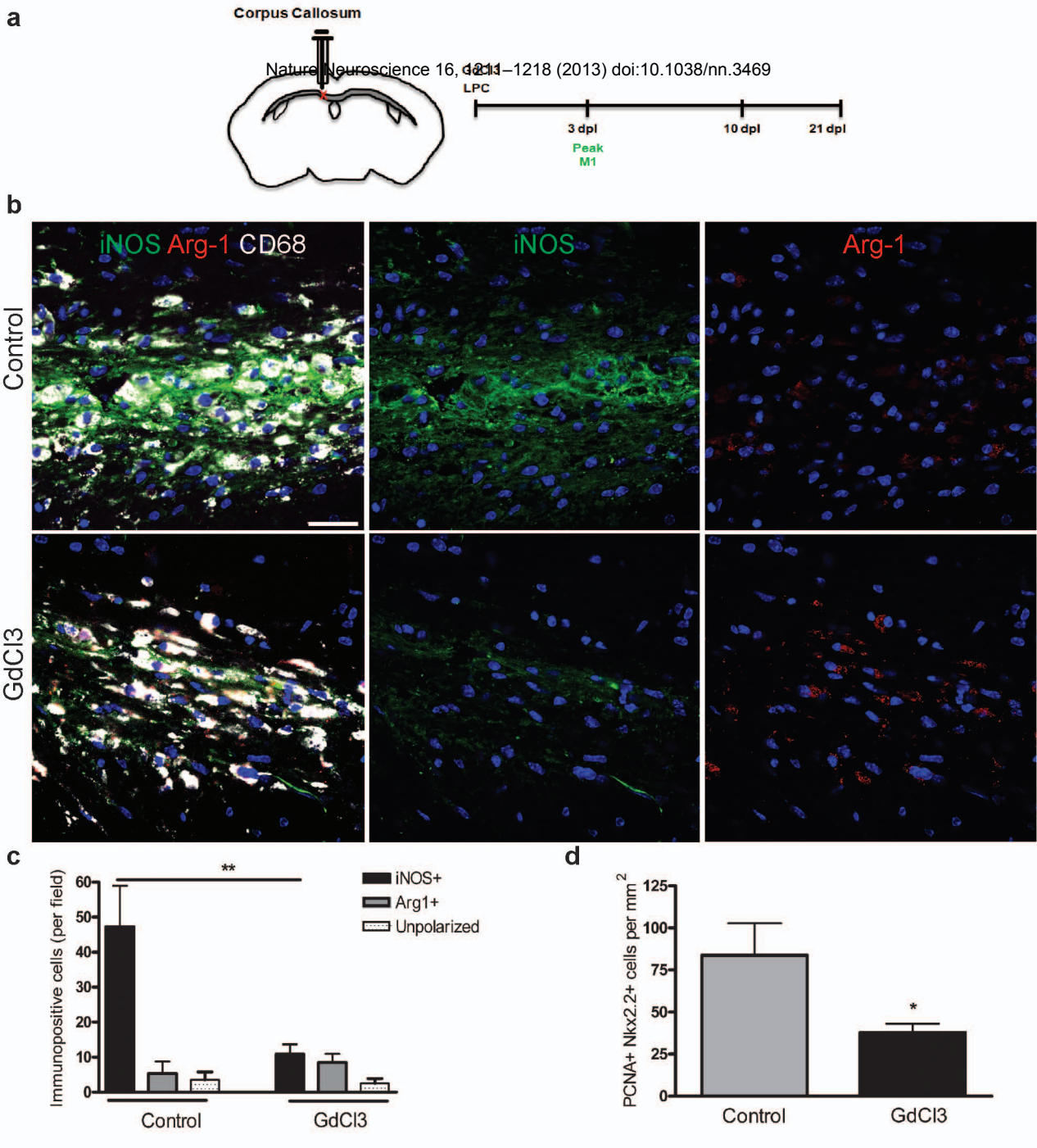

Nature Neuroscience 16, 1211–1218 (2013) doi:10.1038/nn.3469

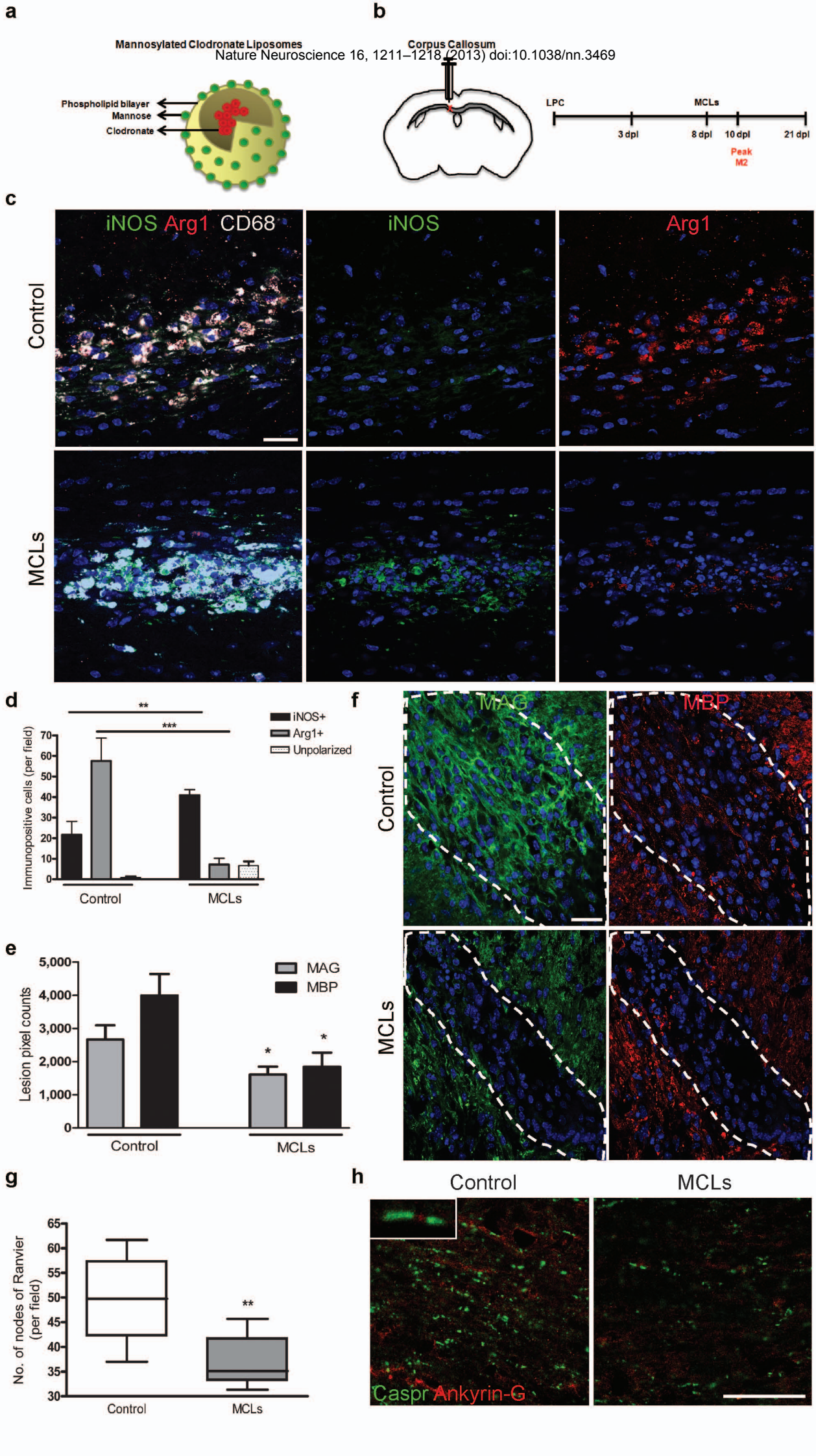

Nature Neuroscience 16, 1211–1218 (2013) doi:10.1038/nn.3469

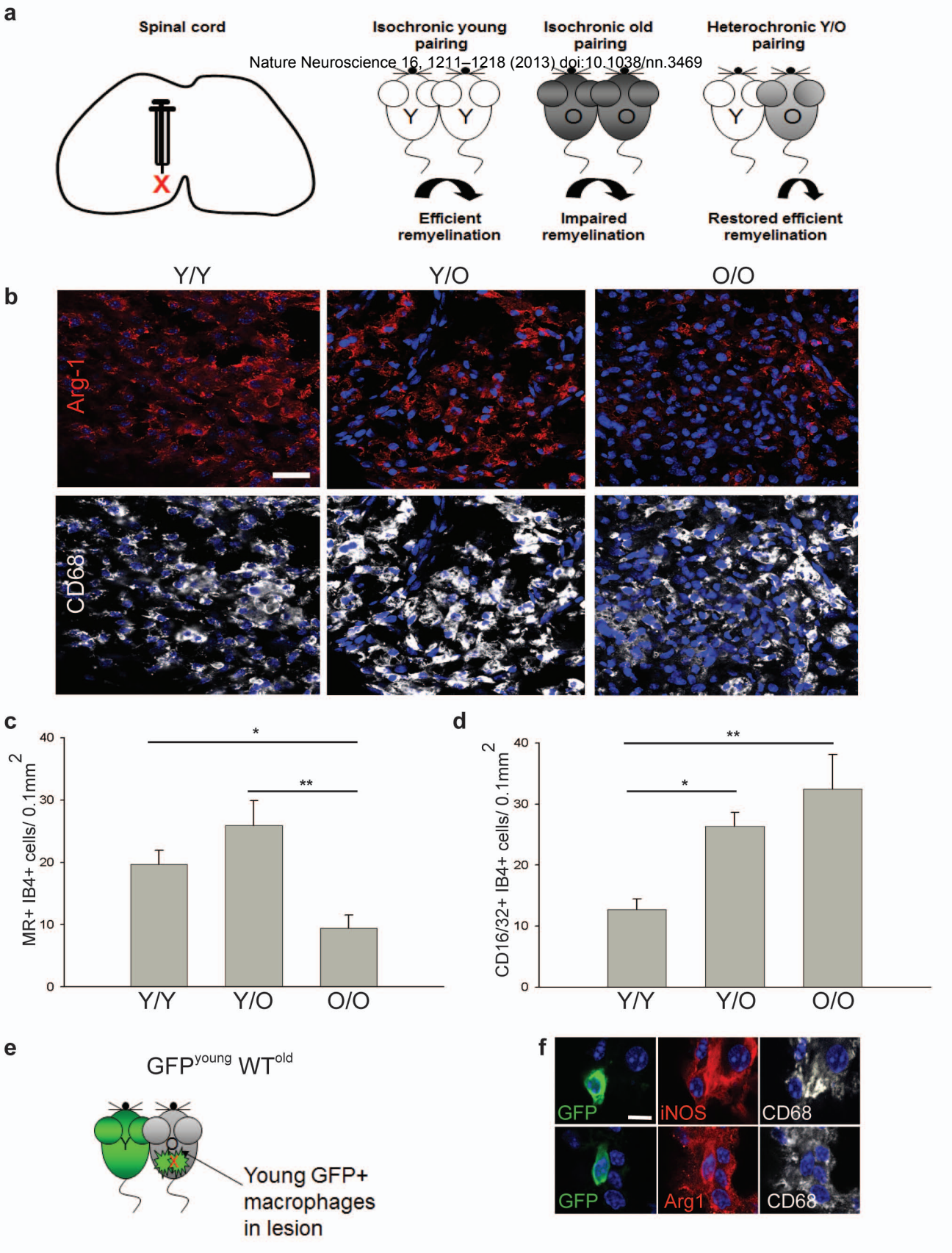

Nature Neuroscience 16, 1211–1218 (2013) doi:10.1038/nn.3469

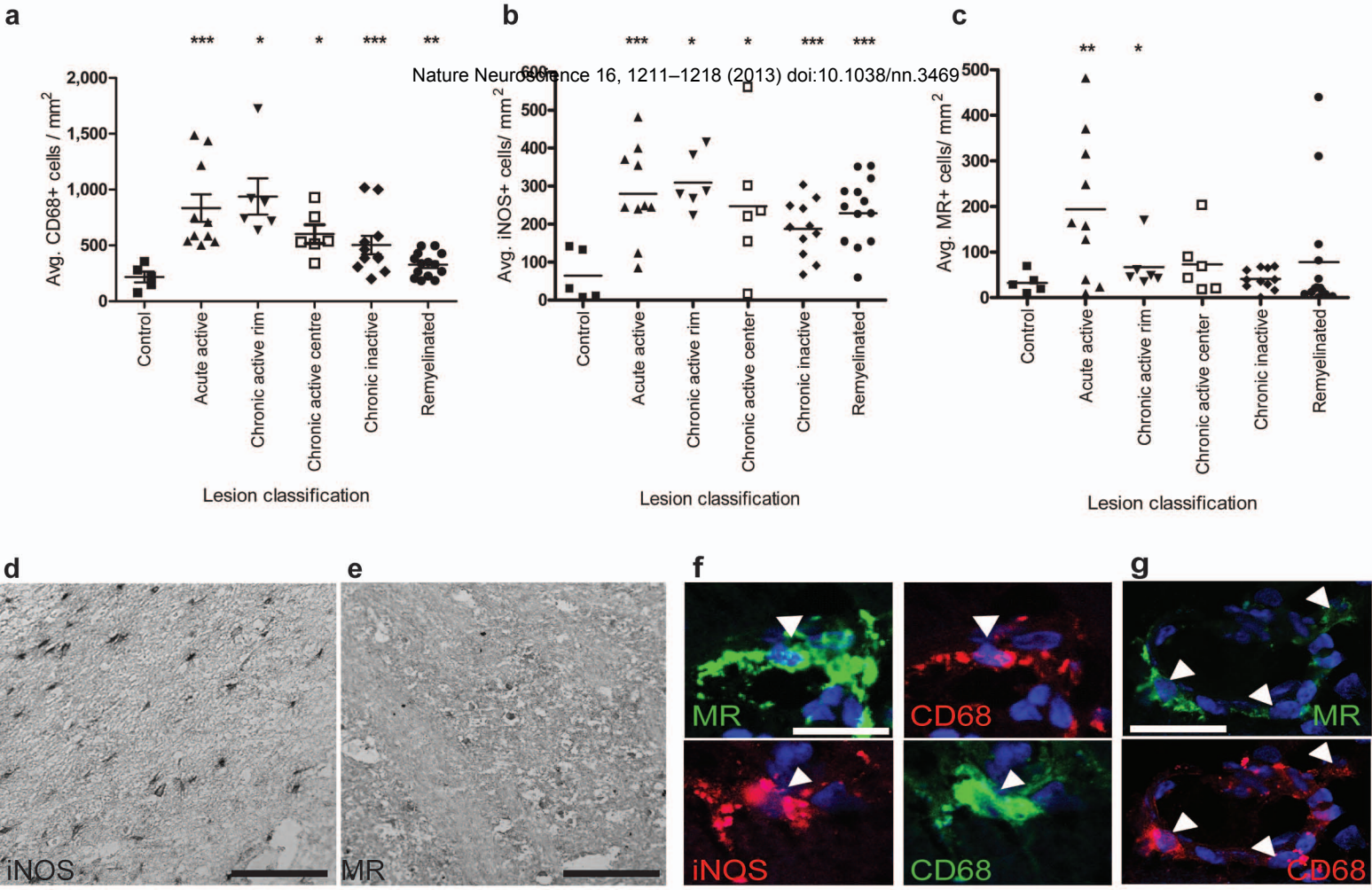

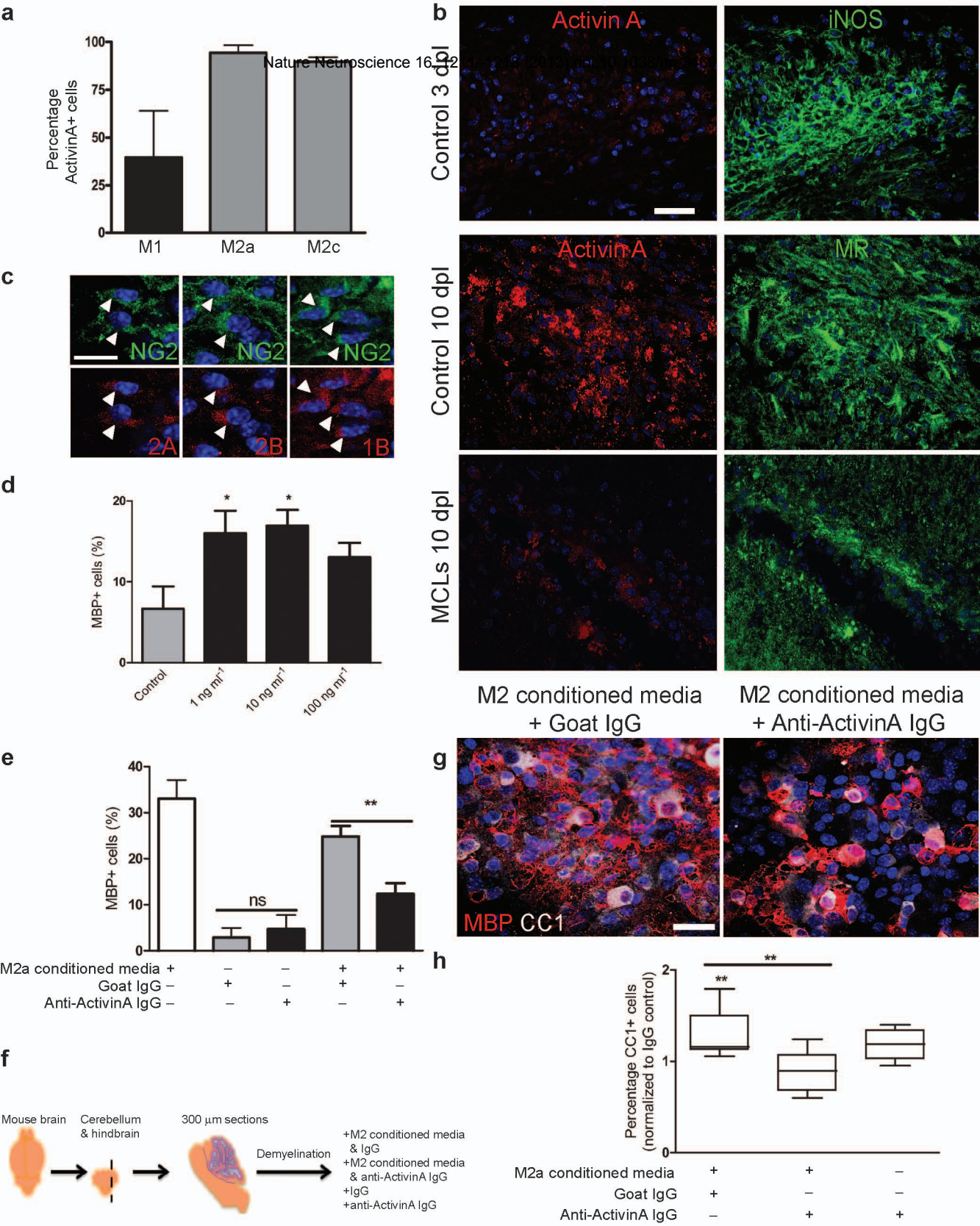
a
Percentage ActivinA+ cells
100
75
50
25
0
M1
M2a
M2c
b
Activin A
iNOS
Control 3 dpl
Activin A
MR
Control 10 dpl
MCLs 10 dpl
c
NG2
NG2
NG2
2A
2B
1B
d
MBP+ cells (%)
20
10
0
*
*
Control
1 ng ml-1
10 ng ml-1
100 ng ml-1
M2 conditioned media + Goat IgG
M2 conditioned media + Anti-ActivinA IgG
e
MBP+ cells (%)
40
30
20
10
0
ns
**
M2a conditioned media + – – + +
Goat IgG – + – + –
Anti-ActivinA IgG – – + – +
g
MBP CC1
h
Percentage CC1+ cells (normalized to IgG control)
2
1
0
**
**
M2a conditioned media + + –
Goat IgG + – –
Anti-ActivinA IgG – + +
f
Mouse brain
Cerebellum & hindbrain
300 μm sections
Demyelination
+M2 conditioned media & IgG
+M2 conditioned media & anti-ActivinA IgG
+IgG
+anti-ActivinA IgG

Nature Neuroscience 16, 1211–1218 (2013) doi:10.1038/nn.3469

Supplemental Information

Title:

M2 microglia/ macrophages drive oligodendrocyte differentiation during CNS remyelination

Authors:

Veronique E. Miron, Amanda Boyd, Jing-Wei Zhao, Tracy J. Yuen, Julia M. Ruckh, Jennifer L. Shadrach, Peter van Wijngaarden, Amy J. Wagers, Anna Williams, Robin J.M. Franklin & Charles ffrench-Constant

Supplementary Figure 1

Nature Neuroscience 16, 1211–1218 (2013) doi:10.1038/nn.3469

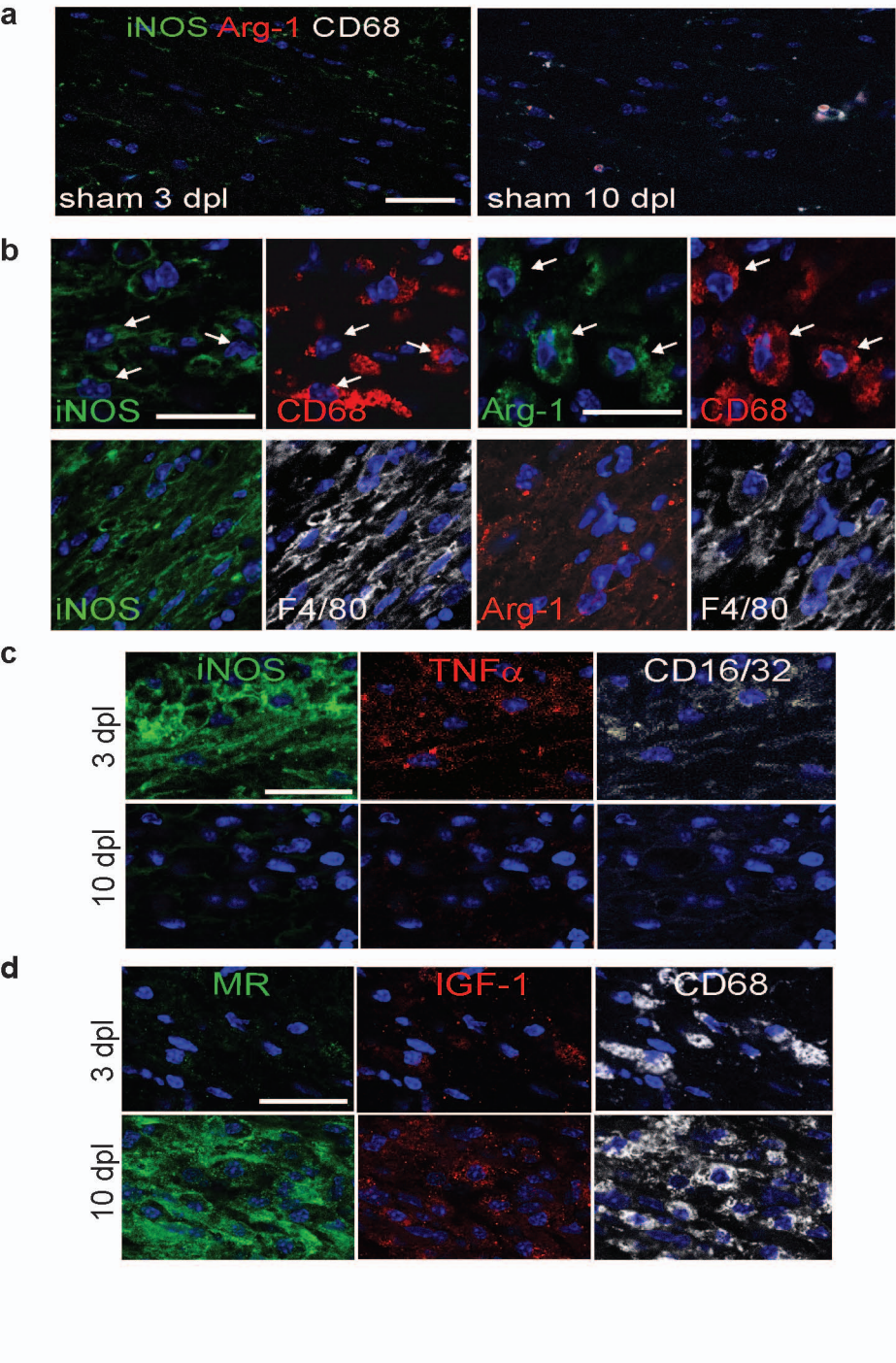

Nature Neuroscience 16, 1211–1218 (2013) doi:10.1038/nn.3469

Supplementary Figure 1 Additional characterization of polarization in corpus callosum lesions.

(a) Representative images of sham PBS-injected lesions at 3 and 10 dpl immunostained for iNOS (green), Arg-1 (red), and CD68 (white). (b) Co-localization of iNOS and Arg-1 in microglia/ macrophage cell bodies (CD68; arrows) and processes (F4/80). 3 and 10 dpl lesions immunostained for additional M1 markers (c; TNFα, CD16/32) and M2 markers (d; MR, IGF-1). All scale bars, 25 μm.

Supplementary Figure 2

Nature Neuroscience 16, 1211–1218 (2013) doi:10.1038/nn.3469

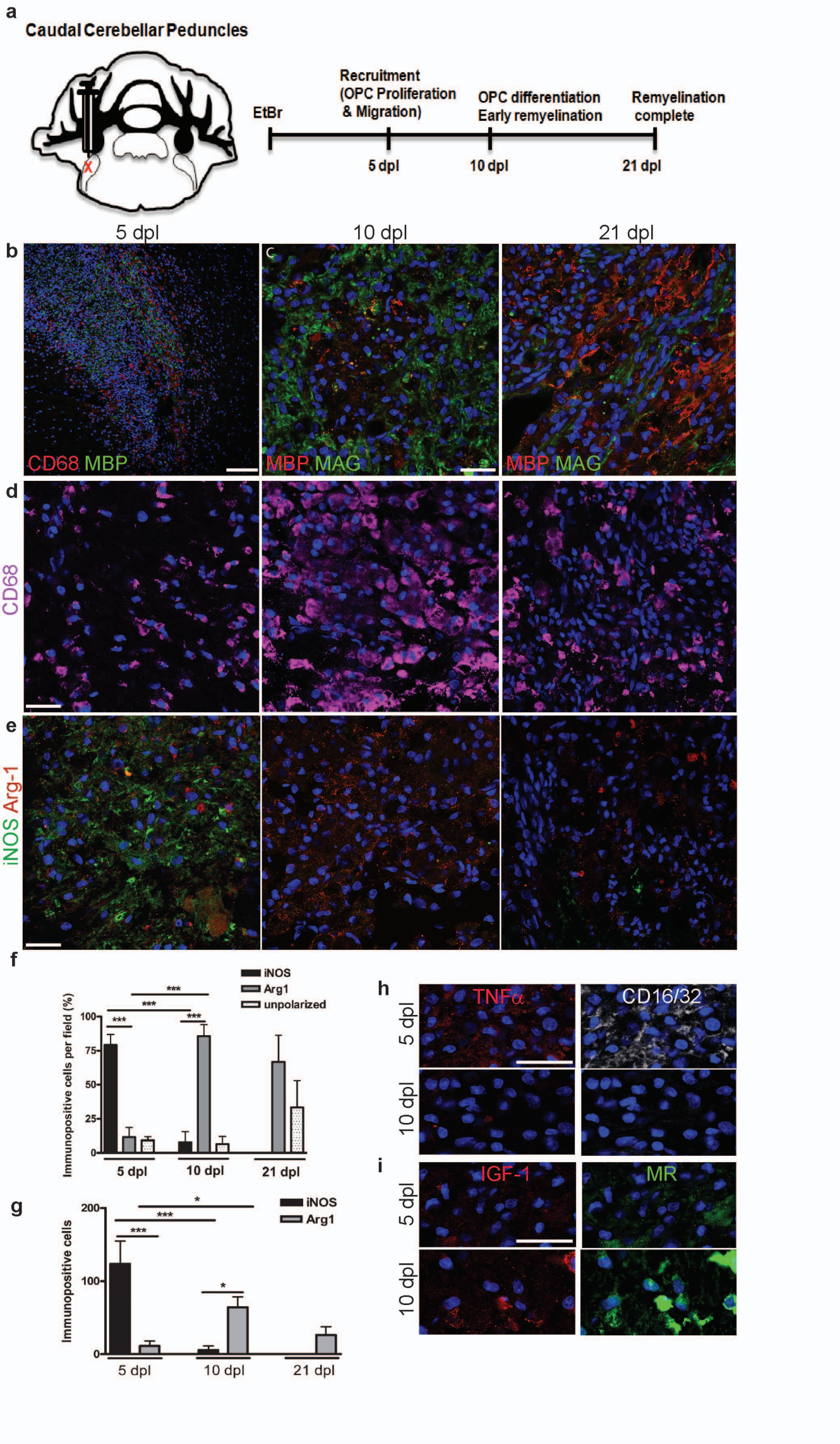

Nature Neuroscience 16, 1211–1218 (2013) doi:10.1038/nn.3469

Supplementary Figure 2 Switch from M1- to M2-dominant response in remyelinating lesions of the rat caudal cerebellar peduncle.

(a) Oligodendroglial lineage cell responses following induction of demyelination of the caudal cerebellar peduncle by stereotaxic injection of ethidium bromide (EtBr). Scale bar, 100 μm. (b) Injection of demyelinating toxin induces accumulation of microglia (CD68+; red) at 5 dpl. Recovery of myelin protein expression is observed with re-expression of MAG at 10 dpl (c, centre) and MBP at 21 dpl (c, right). (d) Microglia/ macrophages (CD68+; purple) are present at 5 dpl, increase in abundance at 10 dpl, and decrease in number by 21 dpl. (e) Representative images of lesions immunostained for iNOS (green) and Arg-1 (red). Percentage (f) and mean number (g) of iNOS+ M1, Arg-1+ M2, and unpolarized (iNOS– Arg1–) cells per field ± s.e.m. at 5, 10, and 21 dpl. One-way ANOVA and Newman-Keuls post test, *$p<0.05$, **$p<0.01$. (n=3, df=26, 17, respectively). (h) 5 and 10 dpl sections immunostained for additional M1 (TNFα, CD16/32) and M2 (IGF-1, MR) markers. All other scale bars, 25 μm.

Supplementary Figure 3

Nature Neuroscience 16, 1211–1218 (2013) doi:10.1038/nn.3469

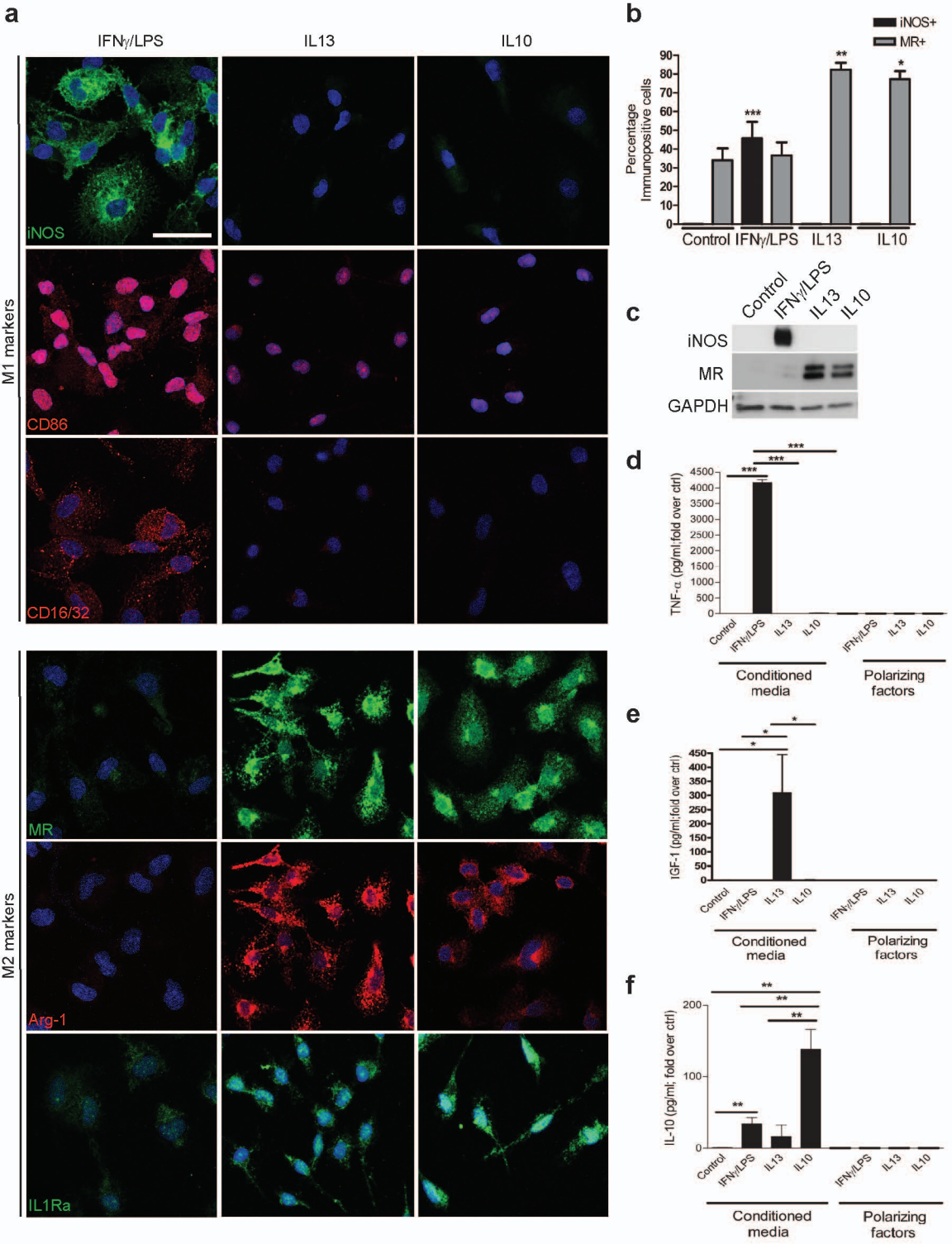

Supplementary Figure 3 Polarization of cultured microglia to M1 and M2 phenotypes.

(a) Representative images of microglia immunostained against M1 markers iNOS, CD86, CD16/32 (top) and M2 markers MR, Arg-1, and interleukin-1 receptor antagonist (IL1Ra) (bottom). Scale bar, 25 μm. (b) Mean percentage of iNOS+ or MR+ cells of total CD68+ cells ± s.e.m.. Kruskal-Wallis test and Dunn's multiple comparison post-hoc test, *p<0.05, **p<0.01, ***p<0.001. (*n*=4) (c) Cropped Western blots showing expression of iNOS with IFNγ/LPS treatment and increase in MR expression with IL-13 or IL-10 treatment, with loading control GAPDH. ELISAs used to assay conditioned media for levels of TNFα (d; *P*=0.0004, *n*=5, df=8), IGF-1 (e; *P*=0.0330, *n*=3, df=4), and IL-10 (f; *P*=0.0051, *n*=5, df=8), presented as mean fold over M0 control ± s.e.m. demonstrating polarization to M1, M2a, and M2c, respectively. A small yet significant increase in IL-10 secretion was observed with IFNγ/ LPS treatment (*P* =0.0081). Polarizing factors alone were included in the assay as a control and did not show detectable levels relative to those measured in conditioned media (d-f). 2-tailed Student's *t*-test.

Supplementary Figure 4

Nature Neuroscience 16, 1211–1218 (2013) doi:10.1038/nn.3469

a

Upregulated M1 genes:	Upregulated M2 genes:
Cd86	*Mrc1 (MR)*
Cxcl11	*Tgfb2*
Ccl2	*Arg1*
Fcgr2a (Cd32)	

b

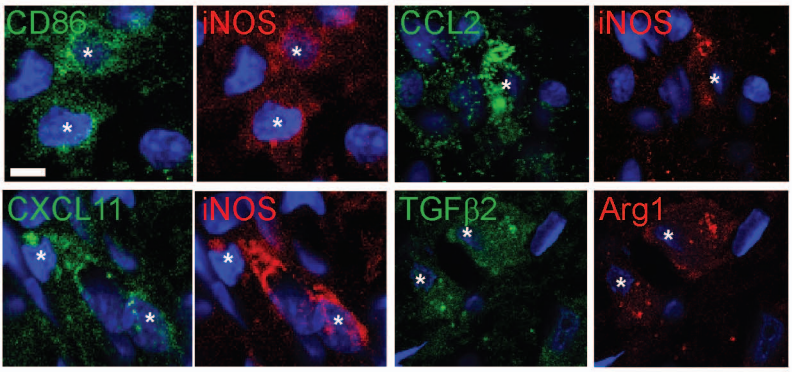

c

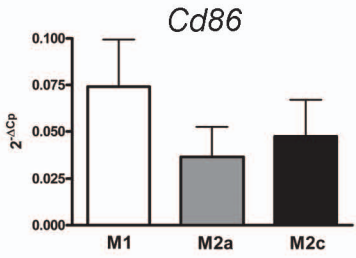

d

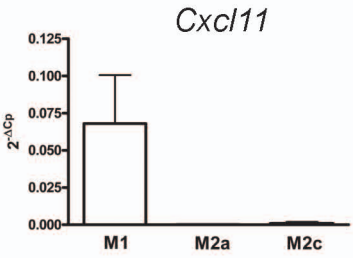

e

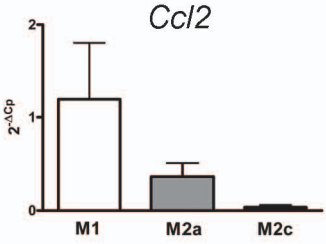

f

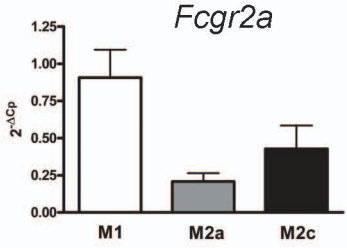

g

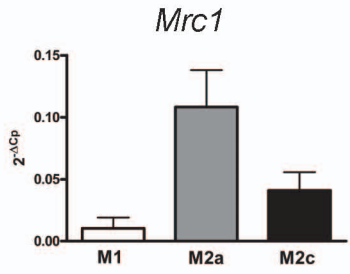

h

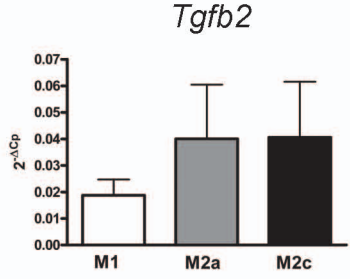

i

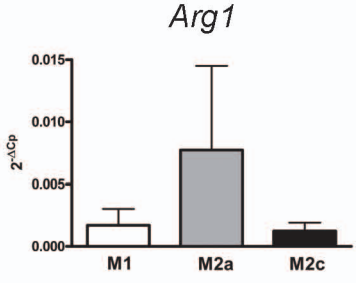

Nature Neuroscience 16, 1211–1218 (2013) doi:10.1038/nn.3469

Supplementary Figure 4 M1 and M2 associated gene expression in cultured microglia.

(a) M1- and M2-associated genes were identified from a previously performed microarray[18] as being significantly upregulated during remyelination of the rat caudal cerebellar peduncles (CCP). These genes were selected for a custom qPCR array to assess gene expression profiles of polarized microglia *in vitro*. (b) Confirmation of expression of additional polarization markers CD86, CCL2, CXCL11, and TGFβ2 in iNOS+ or Arg-1+ cells in the rat CCP. Scale bar, 5 μm. Microglia treated with IFNγ/LPS (M1), IL-13 (M2a), and IL-10 (M2c) were analyzed for gene expression levels of (c) *Cd86*, (d) *Cxcl11*, (e) *Ccl2*, (f) *Fcgr2a* (*Cd32*), (g) *Mrc1*(mannose receptor), (h) *Tgfb2*, and (i) *Arg1*, values are represented as $2^{-\Delta Cp}$ ± s.e.m.

Supplementary Figure 5

Nature Neuroscience 16, 1211–1218 (2013) doi:10.1038/nn.3469

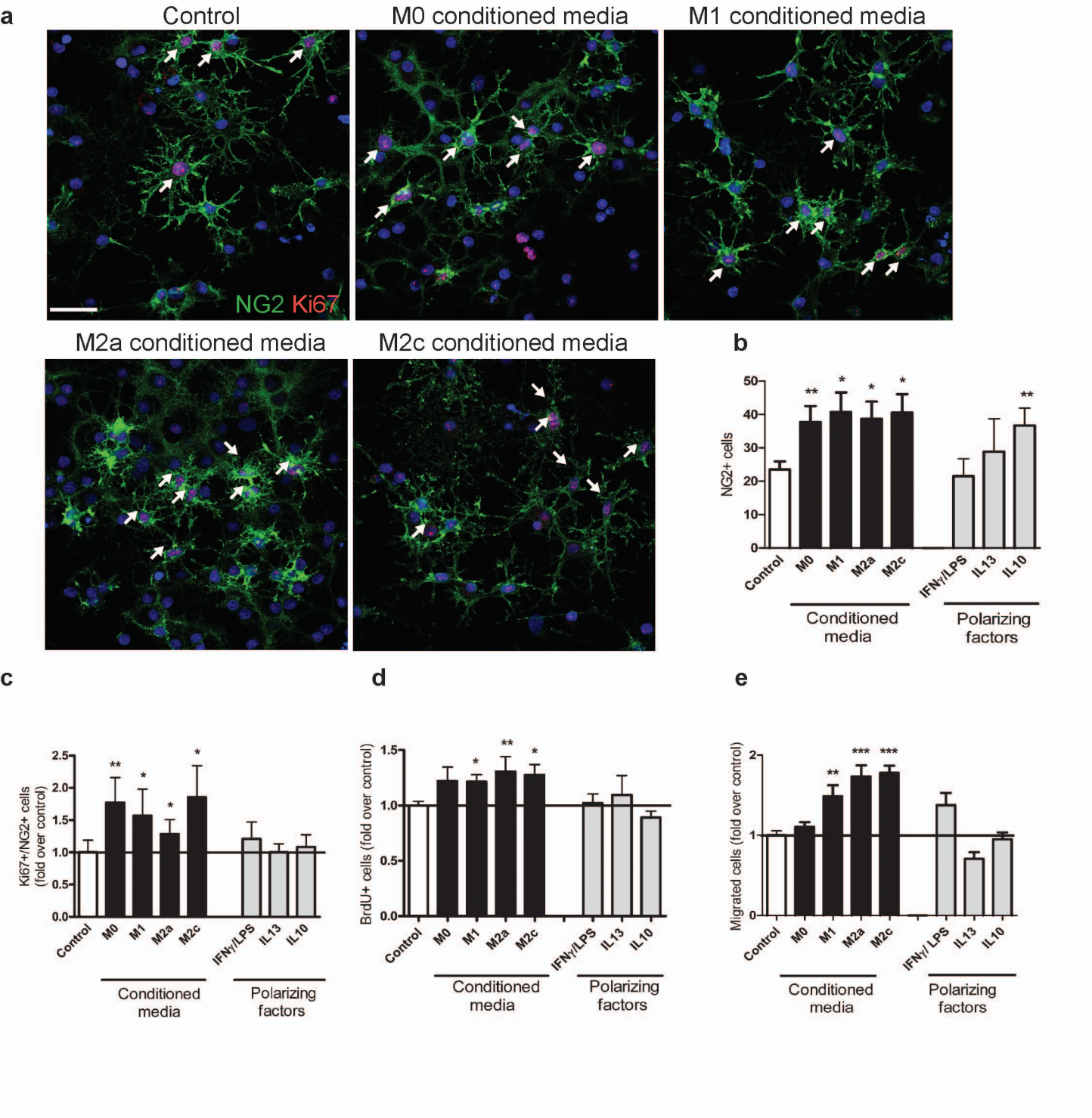

Nature Neuroscience 16, 1211–1218 (2013) doi:10.1038/nn.3469

Supplementary Figure 5 M1 and M2 microglia conditioned media increase OPC proliferation and migration.

OPCs were treated with microglia conditioned media for 3d. Polarizing factors present in the conditioned media (IFNγ/LPS, IL-13, and IL-10) were directly applied to OPCs as a control. (a) Representative images of OPCs immunostained against NG2 (green) and the proliferative marker Ki67 (red). Double-positive cells are highlighted by arrows. Scale bar, 25 μm. (b) Number of NG2+ cells per field was increased with M0 (P=0.005), M1 (P=0.00188), M2a (P=0.00382), M2c (P=0.0119) conditioned media (CM), and IL-10 (P=0.0029) compared to control (n=5, df=8). (c) Ki67+/NG2+ cells were increased with M0 (P=0.0084), M1 (P=0.0362), M2a (P=0.0194), M2c (P=0.0192) conditioned media (n=4, df=6) (d) BrdU+ cells were increased with M1 (P=0.042), M2a (P=0.0083) and M2c conditioned media (P=0.0423) (n=4, df=6). Values from conditioned media-treated conditions (black bars) and polarizing factors alone (grey bars) were normalized to control (unconditioned media, white bars) in (c) and (d), and are represented as mean ± s.e.m., 2-tailed Student's t-test. (e) Number of OPCs ± s.e.m. migrated towards microglia conditioned media (black bars), or polarizing factors alone (grey bars), normalized to values in control (unconditioned media, white bar) showing chemotactic properties of both M1 and M2 conditioned media. Kruskal-Wallis test and Dunn's multiple comparison post-test, **p<0.01, ***p<0.001. (n=3).

Supplementary Figure 6

Nature Neuroscience 16, 1211–1218 (2013) doi:10.1038/nn.3469

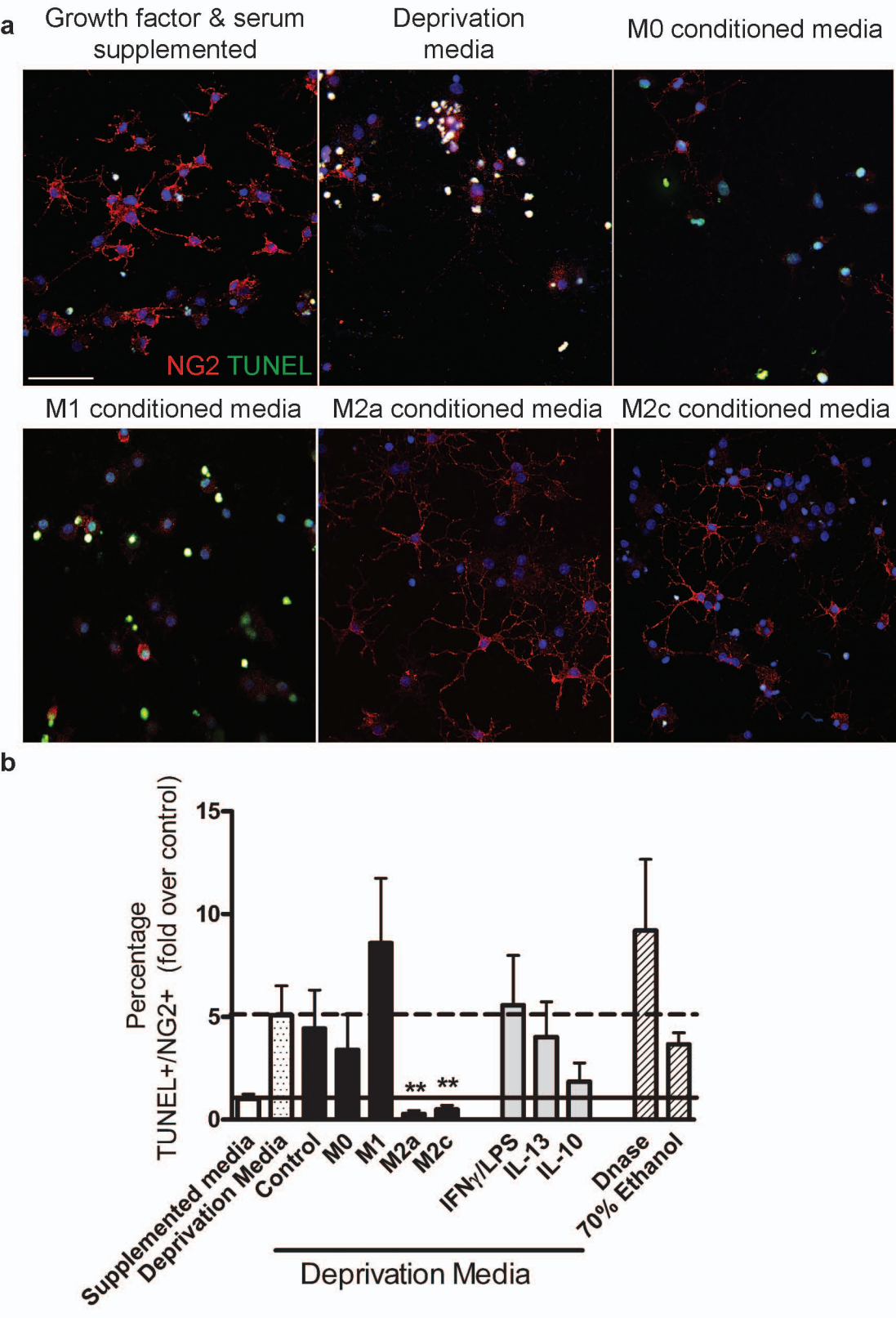

Nature Neuroscience 16, 1211–1218 (2013) doi:10.1038/nn.3469

Supplementary Figure 6 M2 polarized microglia conditioned media promotes the survival of OPCs in a death-inducing environment.

OPCs were treated with microglia conditioned media for 3d in media devoid of serum and growth factors. Polarizing factors present in the conditioned media (IFNγ/LPS, IL-13, and IL-10) were directly applied to OPCs as a control. (a) Representative images of OPCs under basal growth supplemented conditions, grown in deprivation media alone, or supplemented with microglia conditioned media. OPCs were immunostained against NG2 (red) and apoptotic OPCs were visualized by TUNEL assay (green). Scale bar, 50 μm. (b) Mean percentage of TUNEL+ NG2+ OPCs normalized to control supplemented with growth factors and media ± s.e.m.. DNase and ethanol treatment were positive controls for TUNEL positivity. Application of microglia conditioned media to OPCs under normal growth conditions did not induce apoptosis (data not shown). Kruskal-Wallis test and Dunn's multiple comparison post-test, *$p<0.05$, **$p<0.01$. ($n=6$).

Supplementary Figure 7

Nature Neuroscience 16, 1211–1218 (2013) doi:10.1038/nn.3469

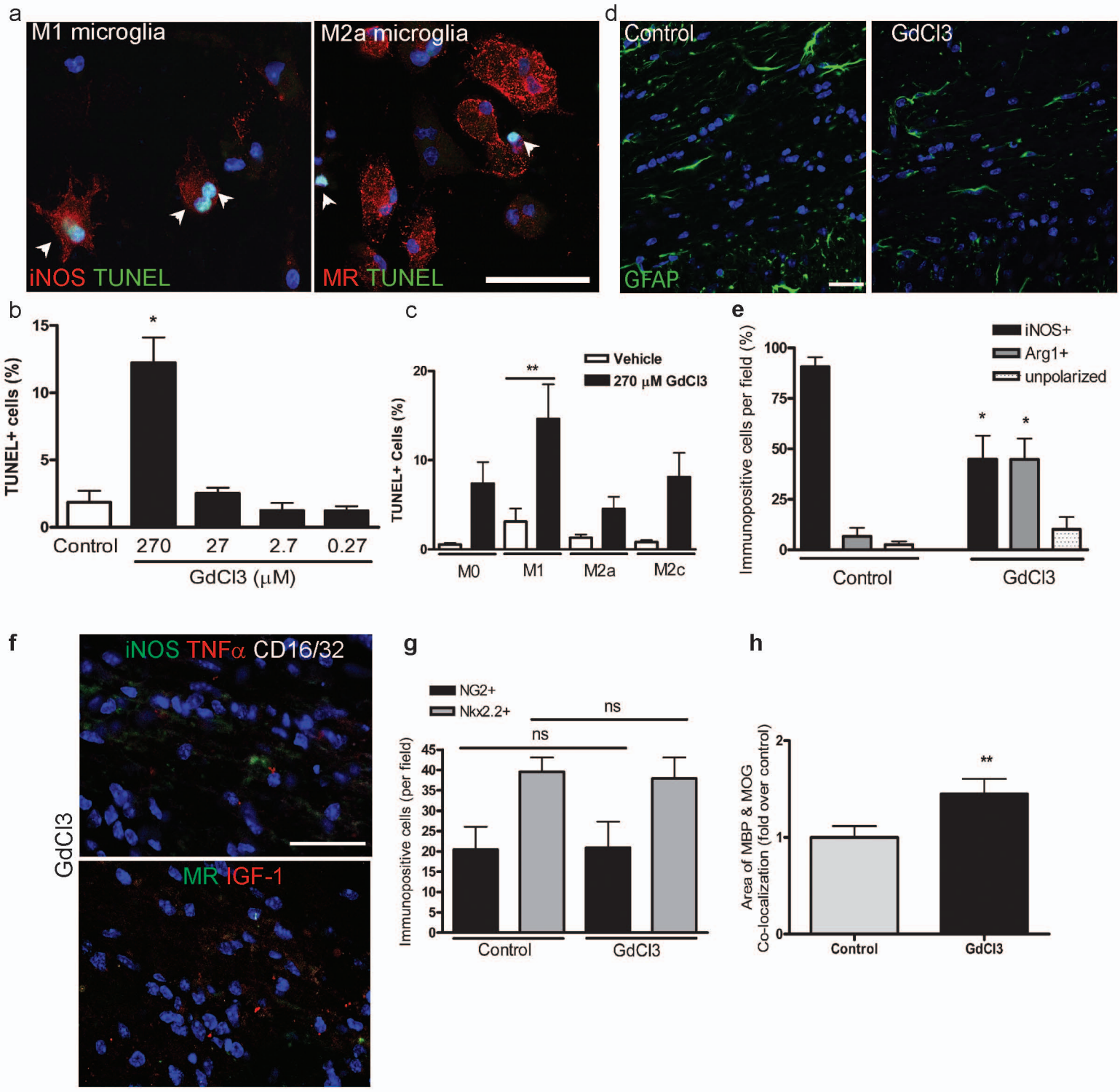

Nature Neuroscience 16, 1211–1218 (2013) doi:10.1038/nn.3469

Supplementary Figure 7 Selective depletion of M1 polarized microglia/ macrophages using gadolinium chloride.

(a) Representative images of M1 (iNOS+; left) and M2a (MR+; right) microglia treated with 270 µm GdCl3 and apoptosis assessed by TUNEL assay (green nuclei). Apoptotic cells are indicated by arrowheads, and were iNOS+ and MR–. Scale bar, 25 µm. (b) Percentage of TUNEL+ M1 microglia treated with vehicle (ctrl), or GdCl3 (0.27-270 µm). Mann-Whitney test, P=0.0286. (n=4). (c) Mean percentage of TUNEL+ cells ± s.e.m. in M0, M1, M2a, and M2c polarized microglia treated with vehicle or 270 µm GdCl3. One-way ANOVA and Newman-Keuls post-hoc test, **p<0.01 (n=6, df=54). (d) GFAP immunostaining in representative control and GdCl3-injected lesions shows no difference in astrocyte reactivity. Scale bar, 25 µm. (e) Percentage of iNOS+ or Arg1+ cells in control or GdCl3-injected lesions, P=0.0135 (iNOS), 0.0319 (Arg1), 2-tailed Student's t-test (n=5, df=8). (f) GdCl3-injected lesions immunostained for M1 markers (iNOS, TNFα, CD16/32) and M2 markers (MR, IGF-1) at 3 dpl. Scale bar, 25 µm. (g) NG2+ (n=4, df=6) and Nkx2.2+ (n=5, df=8) cells per field in control and GdCl3-treated lesions at 3 dpl. 2-tailed Student's t-test, p>0.05. (h) Mean area of MBP and MOG co-localization, fold over control ± s.e.m. in lesions at 21 dpl. P=0.081, 2-tailed Student's t-test (n=6, df=10).

Supplementary Figure 8

Nature Neuroscience 16, 1211–1218 (2013) doi:10.1038/nn.3469

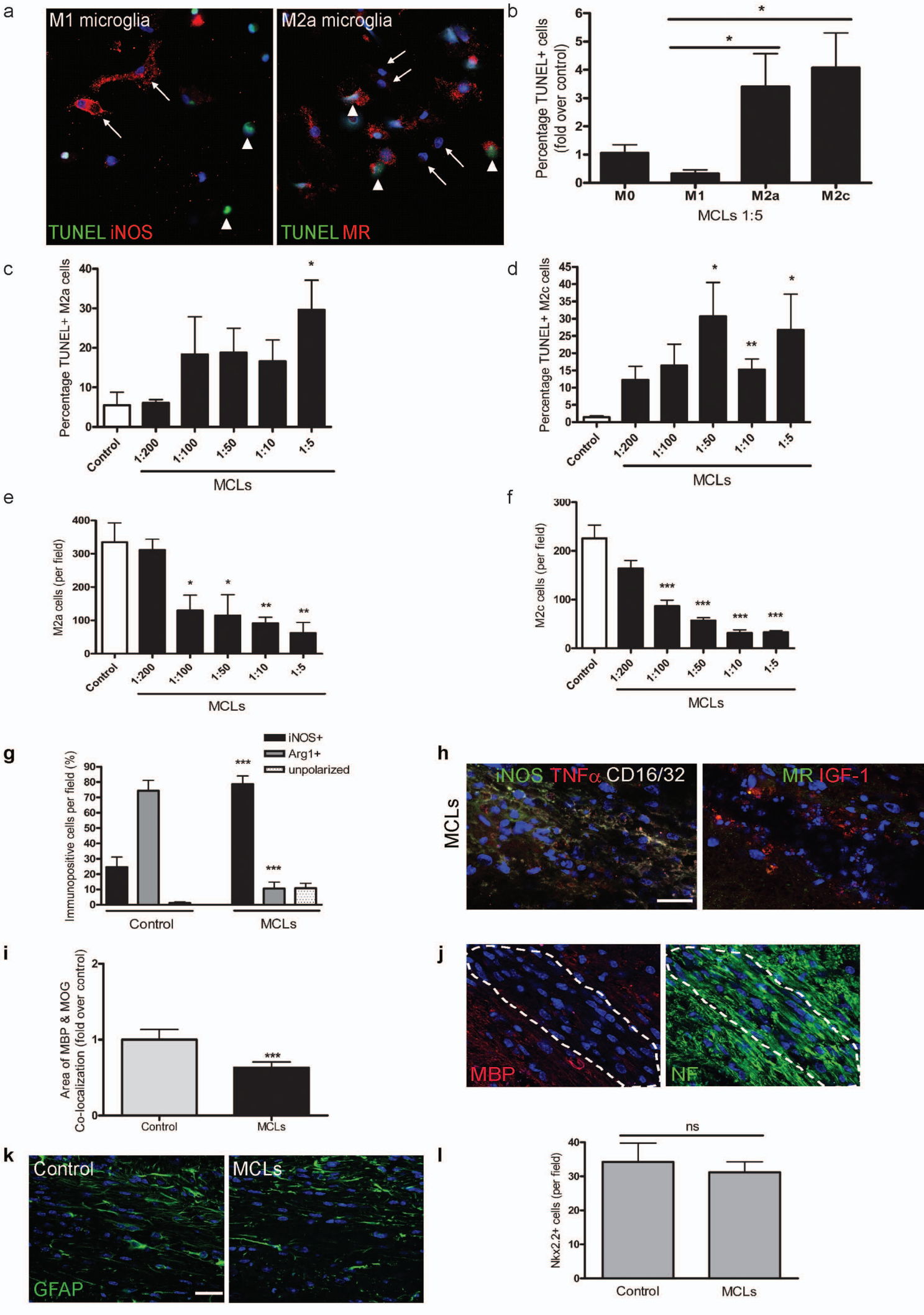

Supplementary Figure 8 Selective depletion of M2 polarized microglia/ macrophages using mannosylated clodronate liposomes.

(a) Representative images of iNOS+ M1 and MR+ M2a microglia treated with MCLs (1:5) and assessed for apoptosis by TUNEL assay. In M1 polarizing conditions, iNOS+ cells were TUNEL– (arrows); TUNEL+ cells were iNOS– (arrowheads). In M2a polarizing conditions, TUNEL+ cells were MR+ (arrowheads), whereas MR– cells were TUNEL– (arrows). (b) Mean percentage of TUNEL+ cells ± s.e.m. in M0, M1, M2a, and M2c polarized microglia treated MCLs (1:5 dilution), normalized to values from M0 conditions. P=0.027 (M1 vs. M2a), P=0.013 (M1 vs. M2c), 2-tailed Student's t-test (n=6, df=10). Mean percentage of TUNEL+ cells ± s.e.m. in M2a (c, P=0.015, df=7) and M2c (d, P=0.0251, 0.0016, 0.03 for 1:50, 1:10, 1:5, respectively, df=6) microglia treated with MCLs (1:200-1:5; black bars) compared to control (white bars) (n=4). Mean numbers of microglia per field ± s.e.m. for M2a (e, P=0.02, 0.03, 0.009, 0.007 for 1:100, 1:50, 1:10, 1:5, respectively, df=6) and M2c (f; P=0.0003, <0.0001, 0.0005, 0.0005 for 1:100, 1:50, 1:10, 1:5, respectively, df=6) polarized cells treated with MCLs (1:200-1:5; black bars) compared to control (white bars), 2-tailed Student's t-test (n=4). (g) Percentage of iNOS+ M1, Arg-1+ M2, or unpolarized (iNOS–, Arg-1–) cells per field ± s.e.m. in control and MCL-injected lesions at 10 dpl. P<0.0001, 2-tailed Student's t-test (n=5, df=8). (h) MCL-injected lesions immunostained for additional M1 (iNOS, TNFα, CD16/32) and M2 markers (MR, IGF-1). Scale bar, 25 μm. (i) Mean area of MBP and MOG colocalization fold over control ± s.e.m. in lesions at 21 dpl. 2-tailed Student's t-test, P=0.0002 (n=6, df=10). (j) Axons (NF+) were detectable running through the lesion (MBP–) at 10 dpl following MCL injection. (k) MCL injection did not influence astrocytes (GFAP+)

within the lesion. Scale bar, 25 μm. (l) Total numbers of Nkx2.2+ OPCs ± s.e.m. in control and MCL injected lesions. 2-tailed Student's *t*-test, p>0.05 (*n*=4, df=6).

Supplementary Figure 9

Nature Neuroscience 16, 1211–1218 (2013) doi:10.1038/nn.3469

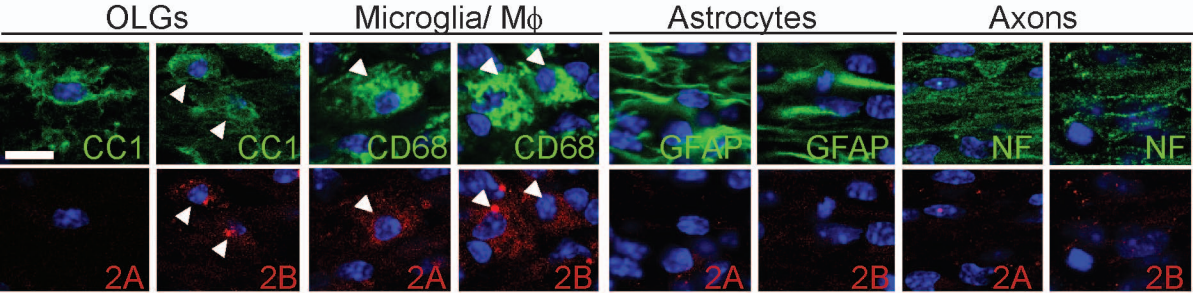

Nature Neuroscience 16, 1211–1218 (2013) doi:10.1038/nn.3469

Supplementary Figure 9 Expression of activin-A receptors on cells in remyelinating lesions.

Representative images of oligodendrocytes (CC1+), microglia/ macrophages (CD68+), astrocytes (GFAP+), and neurons (axons; NF+) with expression (arrows), or lack thereof, of activin-A receptors Acvr2A and Acvr2B. Scale bar, 10 μm.

Nature Neuroscience 16, 1211–1218 (2013) doi:10.1038/nn.3469

Supplemental Table 1. Human brain tissue samples

	Classification	Sex	Age	Disease duration (yrs)	Block	Lesions Analyzed			
						Active	Chronic Active	Chronic Inactive	Remyelinated
Multiple Sclerosis Patients	SPMS	M	46	8	P2E3	0	0	2	2
					P3E3	1	0	1	1
	SPMS	F	49	14	A3D3	3	0	0	0
	SPMS	M	40	9	P3B4	1	0	1	3
	SPMS	F	60	21	P3C3	1	1	1	0
	SPMS	F	34	21	A2D7	1	0	0	0
					A2E2	1	0	1	1
	PPMS	M	37	27	P4D1	0	0	1	3
	SPMS	F	57	27	P3D1	0	0	0	2
	SPMS	F	46	25	A2B3	0	1	1	0
					P2C4	0	2	0	1
	SPMS	F	42	19	A2C2	2	0	0	1
	SPMS	F	57	19	P3C4	0	2	3	0
					TOTAL	**10**	**6**	**11**	**14**
Non-Neurological Controls	Carcinoma of the lung metastasized	M	77	-	P3B4	-	-	-	-
	Cardiac failure	M	64	-	P2D2	-	-	-	-
	Carcinoma of the tongue	M	35	-	P3B3	-	-	-	-
	Ovarian cancer	F	60	-	P3D2	-	-	-	-
	Myelodysplast-ic syndrome, Rheumatoid Arthritis	M	82	-	A2C7	-	-	-	-